Chapter 2. Literature Review

It has long been recognized that polymer crystallization, unlike that of most monomeric substances, occurs under conditions far removed from equilibrium.[1,2,3] Such a behavior is attributed to the long chain length of the polymeric molecules, which makes it difficult for these chains to disentangle from each other in a disorganized and entangled melt, and subsequently for the chains to achieve a regular conformation and align parallel to each other to form an ordered crystal structure. This is the origin of the semicrystalline nature of polymers, since only a fraction of the polymer chains are transformed into crystals under such conditions of restraint. Further introduction of chain irregularities such as branches (in the copolymers studied) reduces the ability of chains to achieve the order required for formation of stable crystals, and thereby suppresses crystallization. Thus the presence of such irregularities strongly influences the mechanism of crystallization and consequently the nature of crystals formed in the copolymers. It is of utmost importance to understand the different mechanisms that operate and the different types of crystal morphologies that are present in these materials. Several theories have been developed with the aim of understanding the crystallization mechanism of the copolymers in comparison to the corresponding homopolymers, and will be discussed in detail shortly. The different types of crystal morphologies possible are also discussed in a later section.

2.1   Models for Semicrystalline Polymers

2.1.1   Fringed-Micelle Model

The fringed-micelle model was one among the earliest morphological models of semicrystalline polymers[1]. This model is based on a two-phase system of crystalline and amorphous regions. The crystalline regions are made up of stacks of short lengths of different chains aligned parallel to each other, while the amorphous regions are

comprised of disordered conformations. The long chain character of polymers allows a given chain to contribute to several different crystalline regions[4] as shown in Figure 1. This model easily accounts for the dissipation of molecular order from the crystalline to the amorphous regions. It also explains the mechanical properties of the samples based on the physical linkages (fringes) between the two regions. However, it is unable to explain the morphological features such as spherulites associated with melt crystallized polymers. These superstructures are accounted for by the chain-folding model as discussed below.

2.1.2   Chain-Folding Model

It was reported by Keller[5,6] that polyethylene single crystals grown from dilute solution appear in the form of thin plates or lamellae when viewed under an electron microscope. These lamellae had thicknesses of ~ 100Å and lateral dimensions of several microns. Diffraction studies on these thin plates revealed that the chain axes are directed more or less perpendicular to the basal faces.[7] Given the extended length of a polymer chain, it was proposed that a chain must traverse a given crystallite many times to conform to both of the above observations. This led to the concept of chain folding in semicrystalline polymers. It was suggested by Keller[6] that the chains traversing a crystallite re-entered the crystallite at adjacent positions by means of hairpin-like bends. Such an adjacent re-entry or regularly chain-folded structure has been demonstrated[8,9] to be predominant in crystallizations from dilute solutions and is schematically depicted in Figure 2.
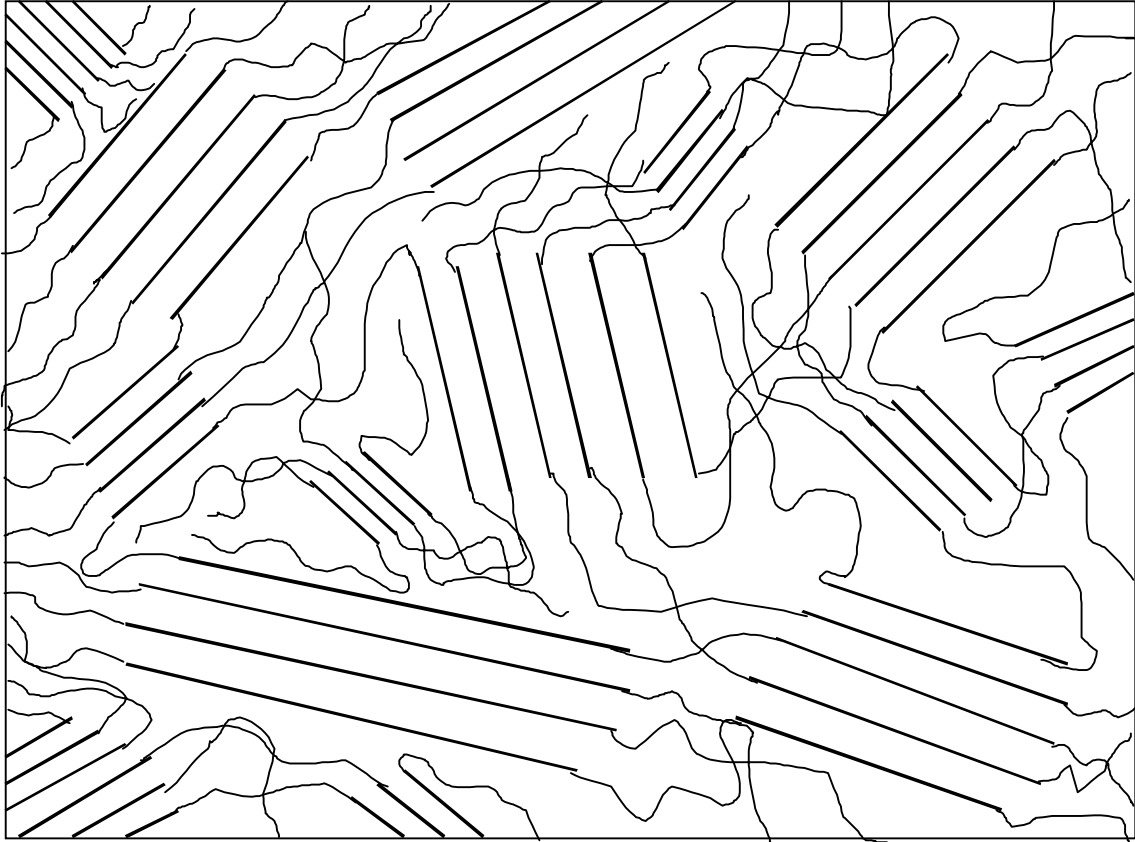
Figure 1 The fringed-micelle model for semicrystalline polymers
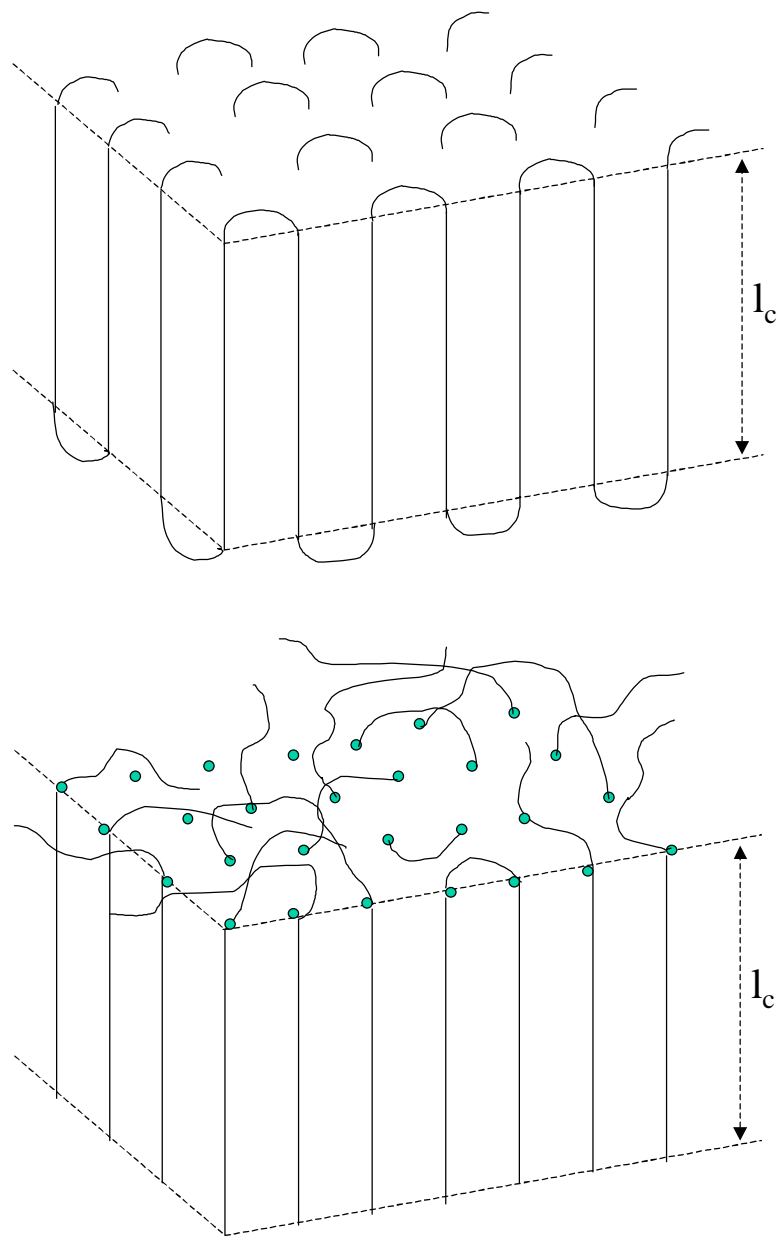(Adopted from Ref. 1).

Figure 2 Regularly folded lamellar structure (top) in comparison to a more random
"switchboard" model (bottom) (Adopted from Ref. 10)

The adjacent re-entry model of Keller was challenged by Flory.[10] In an early theoretical treatment, Flory[10] examined some of the factors related to the generation of a crystalline phase from long chain molecules in random conformations. From the spatial requirements for such chains and a rigorous mathematical treatment, he established that "no more than half of the chains emanating from the lamellar crystal surface can be accommodated by the neighboring disordered amorphous phase". As a result, more than half of those sequences must return to the crystal face from which they departed. This re-entry is proposed to occur via loops of varying lengths that are present in the spaces between the crystal and the amorphous regions. There also exist a number of chains that do not re-enter a given crystallite, but leave the basal plane of the crystal to become part of a disordered amorphous region. These chains could eventually enter another neighboring crystallite. Such a possibility of chain folding often referred to as the "switchboard model" is also depicted in Figure 2. The relative proportions of the ordered crystalline and disordered amorphous regions in a semicrystalline polymer are dependent upon molecular weight, crystallization conditions and presence/absence of chain defects and/or irregularities.

From further theoretical considerations (which are not included here for purposes of brevity), Flory[10] concluded that the regularly folded array is the most stable state for a crystallite in solution under conditions of supersaturation, in contrast to a more haphazard growth expected for melt crystallization. Thus, there is no ambiguity that chain folding in the crystallization of polymers from dilute solutions is highly regular, conforming closely to Keller's model. On the other hand, chain folding in the case of melt crystallization may be between the extremes of a regularly folded arrangement and a random "switchboard" arrangement. The exact nature however, is determined by parameters such as molecular weight, crystallization conditions and the flexibility of polymer chains.

2.2   Morphology of Semicrystalline Polymers

It was mentioned above that polymers form single crystals with regularly chain folded structures when crystallized from dilute solutions. These crystals exhibit thicknesses of ~ 100Å and lateral dimensions of several microns. However, these dimensions are strongly influenced by the solvent, concentration of the solution as well as crystallization conditions.[7] When the polymer concentration is increased to > 0.1% w/v, multi-lamellar structures such as lamellar stacks, sheaves etc. may be formed.

When crystallized from the melt, the lamellae often aggregate together in the form of a superstructure called a spherulite. Spherulites may be viewed as spherical aggregates of lamellae that originate from a common center and radiate outwards as shown in Figure 3. The spherical shape is formed as a result of branching and splaying of lamellae at dislocation points. Typical dimensions of spherulites are of the order of microns and sometimes, even millimeters. Therefore, they can be easily viewed under an optical microscope. The spherulites continue to grow radially until they impinge upon one another. A measure of their growth rate until the time of impingement provides a wealth of information regarding the mechanism of crystallization in the polymer, and has been the focus of several investigations.

The two types of morphologies discussed above are usually developed during the crystallization of polymers under quiescent conditions. However, crystallization under flow could result in other morphological forms such as a "shish kebab" structure. Since the present study is only concerned with quiescent crystallization, these other structures are not discussed in detail here. However, they are highly relevant to polymer processing applications.

The above discussion is only a brief summary of the different crystal morphologies possible in semicrystalline polymers. It is by no means a comprehensive description of the topic. A more detailed and complete picture of polymer morphology has been given by Woodward.[11]
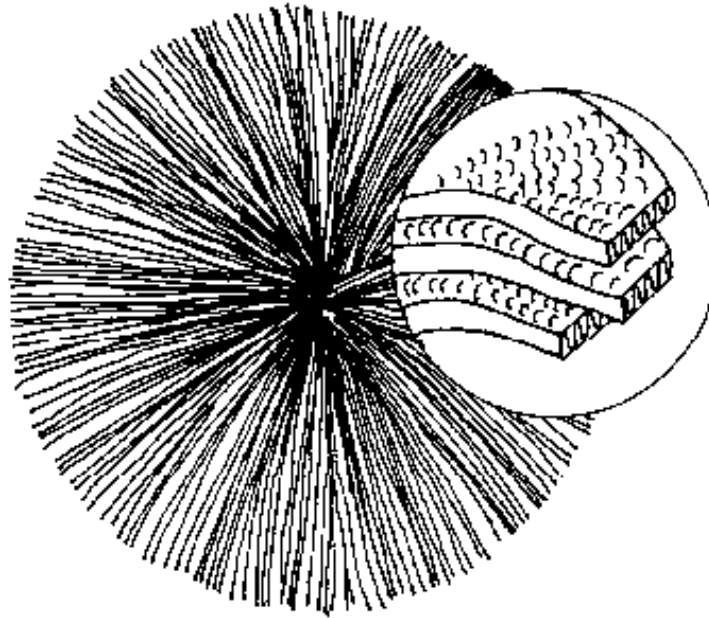
Figure 3 A polymer spherulite with chain folded lamellae. The branch points are also indicated (Adopted from Ref. 7).

2.3   Secondary Crystallization

The process involving the formation of a spherulitic superstructure may be roughly classified as primary crystallization. However, it has been widely reported that the physical and mechanical properties as well as the degree of crystallinity of many polymers continue to vary considerably with time, after the completion of this step. The process involving the time-dependent evolution of the crystallinity of the material (subsequent to the completion of primary crystallization) is termed as secondary crystallization. It may be viewed as a slow process of completion of the crystallization process in polymers and has been demonstrated to have immense implications on the time-dependent properties of polymers.

Several mechanisms have been proposed for the secondary crystallization in semicrystalline materials. For highly crystalline polymers such as linear polyethylene (LPE), the long time evolution of crystallinity has been associated with a lamellar thickening process.[12,13,14] Furthermore, it has been shown to follow a log-time kinetics.[15,16,17,18,19] Schultz and Scott[12] and Collins[20] have also reported that the rate of increase of crystallinity with log time increases with temperature, suggesting a mobility-controlled process. However, all the above studies are limited in scope because the thickening process is only operative above the α-relaxation temperature of highly crystalline polymers and only a few polymers such as LPE, PEO, i-PP, POM and PVF_2 exhibit such a relaxation.

The mechanism of the temporal evolution of properties is much less understood for polymers with relatively lower crystallinities (compared to LPE). These materials crystallize much more slowly than LPE, and exhibit significant variations in properties with long term annealing. For polymers having bulky unit structures such as PET, nylons, PEEK, i-PS, PC, PBT, PVC etc. and for copolymers with branches along the backbone, the lamellar thickening process may be dismissed as being highly unfavorable on the basis of the reorganization required at the lamellar fold surface.

Several other mechanisms such as generation of new lamellae[21], crystal perfection[22,23], and a combination of thickening and recrystallization[24] have also been proposed for secondary crystallization. The exact nature of the process involved depends

on factors such as chain mobility, stiffness of chains, level of primary crystallinity, degree of constraint in the amorphous regions etc. An examination of the true nature of this process is essential for the understanding of the long-term properties of semicrystalline polymers, especially of the type mentioned in the previous paragraph.

2.4   Crystallization Behaviors of Homo- and Copolymers of Ethylene

Before proceeding to the details of the theories of crystallization for homo- and copolymers (of ethylene), it is useful to point out the major differences between their crystallization behaviors. The purpose of such a discussion at this point is to prepare the ground for a better understanding of the details (theories and relevant literature) that are presented subsequently.

A typical homo- and copolymer of ethylene are schematically depicted in Figure 4. Unlike a homopolymer, a copolymer is fragmented into a number of sequences by the occurrence (the frequency of occurrence is dictated by the branch concentration) of branches along the backbone. In polyethylene, the branches are almost always (except for the methyl) excluded from the crystal structure formed. [This aspect will be elaborated upon in the following section]. As a result, the copolymers display a wide range of sequence lengths that can crystallize over a correspondingly wide range of temperatures. This feature forms the basis of most of the differences observed in the crystallization behaviors between the homo- and copolymers.

The crystallization of homopolymers is largely influenced by the chain length and its distribution, the extent of entanglement of chains in the melt and the undercooling. However, that in copolymers is predominantly influenced by the crystallizable sequence length distribution, which in turn is determined by the branching statistics. The branching statistics in polyethylene copolymers is governed by the nature of the catalyst used.
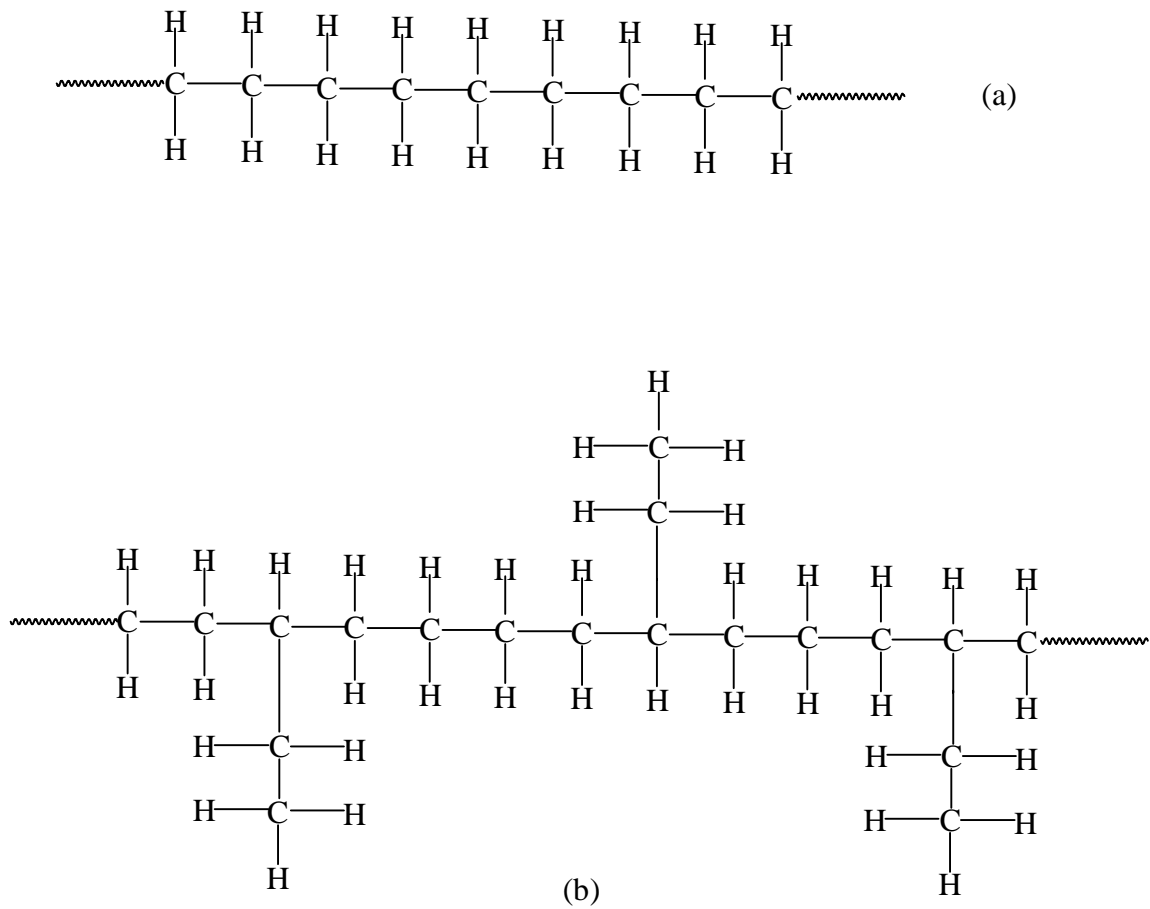
Figure 4 Schematic representation of (a) linear polyethylene and (b) ethylene/1-butene copolymer (Adopted from Ref. 2)

When a homopolymer is crystallized from the melt, the thickness and melting temperature, T_m, of the crystals formed are dictated by the undercooling, $(T_m - T_c)$. The lower the crystallization temperature, T_c, the larger is the driving force for crystallization. This leads to rapid formation of crystals from the melt - these crystals are thinner and melt at lower temperatures. When crystallized at higher temperatures, the chains have sufficient time to rearrange expeditiously to form thick and stable crystals that have higher melting temperatures. As mentioned earlier, the long term annealing of polymer chains can result in their rearrangement leading to thicker crystals by means of lamellar thickening (it is one of the possibilities during secondary crystallization). It may be recalled that thickening can occur only at temperatures higher than the α-relaxation temperature (if present), $T_{\alpha c}$, of the material.

It is possible to crystallize all the chains available at a specified temperature, provided sufficient time is allowed for this process to be completed. [This is practically not very feasible because the times involved can be unreasonably long]. It must also be mentioned that at very low temperatures, the driving force for crystallization is superseded by the decreased mobility of the chains, owing to the closeness to the glass transition temperature (T_g). At these temperatures, the rate of crystallization decreases. This difficulty is not encountered in linear polyethylene because of its low T_g and its tendency to crystallize at relatively low undercoolings.

The crystallization in copolymers is markedly different from the above mechanism. Sequences of varying lengths (determined by branch frequency) are present. These sequences can only crystallize below certain temperatures, determined by their lengths. As a result, the sequence length, and not the undercooling is the dominating factor. Then it is clear that it is not possible to crystallize all of the chains at a given crystallization temperature. In other words, the crystallinity of a copolymer continues to increase significantly with decreasing temperature. This is in contrast to the crystallinity of a homopolymer (more specifically linear polyethylene), which exhibits a comparatively insignificant increase. It also follows from the difference noted above that a broad range of melting temperatures may be expected for the copolymers.

The crystallization process in copolymers is further influenced by the fact that branches longer than the methyl are predominantly excluded from the growing crystal.

This leads to crowding in the amorphous regions due to the accumulation of branched units. As a result, the crystals formed under such conditions are much thinner and less perfect compared to those formed from the corresponding linear material. Thus, the crystal forming process in copolymers is largely dominated by kinetic factors such as chain transport and mobility.

The above discussion illustrates the fundamental differences between the crystallization behaviors of homo- and copolymers (of ethylene). Due to the reasons outlined above, the crystallization process in copolymers is much slower than that in a homopolymer. As a result, there is a considerable increase in the level of copolymer crystallinity at long times. This increase is accompanied by time-dependent variations in other physical and mechanical properties as well as in the structure and morphology of the materials. These ideas may be elegantly explained by invoking the concept of secondary crystallization that was discussed in Section 2.3 above. It is essential to have a complete understanding of the changes in structure at the molecular level that result in the observed time dependence of the properties. It is also useful in making meaningful predictions about a specific property at prolonged times in order to be able to successfully manipulate the end-use of the materials involved. The present study is aimed at gaining such an understanding by investigating the temporal evolution of secondary crystallization in random ethylene/α-olefin copolymers. The above discussion also provides a means of justification for the need to carry out the present investigation.

2.5   Crystallization Theory of Homopolymers

2.5.1   Flory's Crystallization Theory for Homopolymers

Flory's theory[25] for the crystallization of homopolymers is based on a linear polymer comprised of x identical structural units, A, that enter a hypothetical lattice, some of whose cells are occupied by solvent molecules. [Although the present study is not concerned with polymers in dilute solution, Flory's model (involving a solvent) is presented here, since it forms the basis for the understanding of further treatments for copolymers. Moreover, predictions in the absence of a solvent can be made by equating

the volume fraction of solvent to zero]. This lattice is used to model a crystal in equilibrium with its amorphous phase. The relationship between equilibrium crystallite length, ζ_e, and other modifiable parameters as predicted by this treatment is shown below.

(1)
$$-\ln(v_2 D) = \frac{\varsigma_e}{x - \varsigma_e + 1} + \ln\left[\frac{x - \varsigma_e + 1}{x}\right]$$
$$\cong \frac{1}{x} + \left(\frac{1}{2}\right)\left(\frac{\varsigma_e}{x}\right)^2 + \left(\frac{2}{3}\right)\left(\frac{\varsigma_e}{x}\right)^3 \ldots\ldots$$

where v_2 = the volume fraction of polymer, and

$$D = \exp\left(\frac{-2\sigma_e}{RT}\right)$$

where σ_e = the fold surface free energy per unit area.

It follows from Equation (1) that ζ_e increases with a decrease in either v_2 or D. The increase in crystallite length with increasing dilution of the polymer solution (decreasing v_2) can be explained on the basis of the increased mobility of the chains, affording easier diffusion of these chains to the growing crystallite surface. A decrease in D implies fewer growing centers competing for a given chain, thereby increasing the possibility of the chain being added to an already growing crystallite. These predictions are in accordance with experimental observations, although the equilibrium crystallite length proposed by Flory may never be achieved in reality, due to the restrictions placed on chain motion in actual polymers.

The variation of ζ_e with chain length, x, is derived from the series expansion shown in Equation (1). As expected, ζ_e is found to be directly proportional to chain length, for large values of x. For such large chain lengths, the crystallite length, ζ, is related to the melting temperature, T_m, as predicted by the following relationship.

(2)
$$\frac{1}{T_m} - \frac{1}{T_m^0} = -\left(\frac{R}{h_u}\right)\left(\frac{\ln D}{\varsigma}\right)$$

where T_m^0 = the melting point of the pure polymer of infinite chain length, and

      h_u = the heat of fusion per structural unit.

It then follows that the depression in melting point below T_m^0 varies inversely as the crystallite length. At a given temperature, crystallites of length, ζ, with a melting temperature, T_m, are formed until all the chain sequences that can be possibly involved in such a process have been exhausted. Further continuation of this process would result in excessive strain on the residual amorphous phase, owing to distortions and loss of entropy. However, crystallites of shorter lengths with a further depression of melting temperature can be formed upon decreasing the temperature. Thus, a breadth of crystallization and melting temperatures results, depending on the extent of departure from the infinitely thick equilibrium crystallite. These observations further imply that the equilibrium assumptions of Flory are far removed from the actual behavior observed.

A similar expression[25] for the variation of depression in melting point with chain length, x, is also derived and is given by:

$$(3) \qquad \frac{1}{T_m} - \frac{1}{T_m^0} = \left(\frac{R}{h_u} \right) \left(\frac{1+b}{x} \right)$$

where b $\propto$ (ζ_e - 1) / x, and is approximately a constant for large x.

From this expression, it is seen that crystallites with higher melting temperatures are formed from longer chains. Such a prediction is in compliance with the variation of melting point depression with crystallite length noted above, since larger crystallites are expected to melt at higher temperatures.

So far, we have discussed the crystallization theory of homopolymers developed by Flory. Most of the predictions based on this theory are in accordance with experimental observations.[26] However, some deviations are also noted, due mainly to the assumptions of equilibrium. For instance, the infinite crystal and the sharp melting and crystallization transitions, as predicted by the theory may never be achieved experimentally.

2.5.2   The Kinetic Theory of Crystallization for Homopolymers

Lauritzen and Hoffman[27,28,29,30,31] have developed an elegant theory for polymer crystallization based on the concept of a kinetically controlled process. [This theory is also appropriately referred to as the kinetic theory of polymer crystallization]. According to this treatment, the crystallization range of a polymer is divided into three regions or Regimes that are dictated by the rates of two processes, namely secondary nucleation and lateral spreading or growth. The rates of these processes are represented as i and g respectively. Then, the three regimes of crystal growth occur when:

$$g \gg i \qquad \text{Regime I}$$
$$g \approx i \qquad \text{Regime II}$$
$$g \ll i \qquad \text{Regime III}$$

In Regime I, a single nucleus is formed on a surface and crystal growth continues by the lateral spreading of a single crystalline patch. In Regime II, several nuclei are formed simultaneously and spread along the surface to give rise to new crystalline layers. In Regime III, the secondary nucleation rate is so fast that it supersedes any lateral spreading along the crystal surface resulting in an uneven fold surface, approaching the limiting case of Flory's switchboard model.

The free energy of fusion, ΔG_f, for a polymer crystal given by the above treatment is shown below:

(4) $$\Delta G_f = xyl\Delta G_f^{\infty} - 2xy\sigma_e - 2l(x + y)\sigma$$

where ΔG_f^{∞} = the free energy of fusion per unit volume for an infinitely large crystal

σ_e = the fold surface free energy per unit area

σ = the lateral surface free energy per unit area, and

x, y and l = the length, breadth and thickness of the crystal respectively.

In the case of an infinitely large and perfect crystal, for which the surface effects represented by σ and σ_e can be neglected, Equation (4) can be re-written as:

$$\Delta G_f = xyl\Delta G_f^\infty = xyl\left(\Delta H_f^\infty(T) - T\Delta S_f^\infty(T)\right)$$

At the equilibrium melting temperature, T_m^e, $\Delta G_f^\infty = 0$. As a result, the melting temperature of such a crystal can be expressed as:

$$(5) \qquad T_m^e = \frac{\Delta H_f^\infty(T_m^e)}{\Delta S_f^\infty(T_m^e)}$$

The melting temperature, T_m, of a smaller crystal is obtained by substituting Equation (5) in Equation (4). Furthermore, for such a crystal, the following approximations can also be made: $\sigma \ll \sigma_e$ and x, y $\gg$ l. Then, T_m is given by:

$$(6) \qquad T_m = T_m^e\left(1 - \frac{2\sigma_e}{l\,\Delta H_f^\infty}\right)$$

This expression is called the Gibbs-Thomson-Tammann[32,33] equation. More specifically, it is the variant of the Gibbs-Thomson equation for a crystal of large lateral dimensions and finite thickness.

The Lauritzen-Hoffman theory also predicts that the initial lamellar thickness, l_g^*, of a polymer crystal is related to the extent of undercooling, ΔT, as,

$$(7) \qquad l_g^* = \frac{2\sigma_e T_m}{\Delta H_f^\infty \Delta T} + \delta l$$

where δl = an increment in stem length, and is weakly temperature dependent.

During isothermal crystallization of certain polymers (such as LPE), the crystal thickness increases to larger values. Although lamellar thickening is a thermodynamically favorable process leading to the reduction of surface free energies of the crystals, it is not a universal phenomenon for all semicrystalline polymers. It is not

observed in polymers such as PET, *i*-PS, PC, PEEK, PBT etc. with stiff backbone structures and/or bulky groups. It is also unlikely to occur in copolymers where the backbone is frequently interrupted by branches of different lengths. The absence of the thickening process is related to the absence of the α_c-relaxation process (process involving the onset of chain mobility in polymer crystals, characterized by a temperature, $T_{\alpha c}$) in these polymers. Since thickening requires a fair degree of chain mobility within the crystals, it can occur only above $T_{\alpha c}$ in polymers that exhibit such a relaxation.

It has also been suggested that the lamellar thickening process could be related to the crystallization regimes.[34] This correlation is based on the roughness or irregularity of the fold surface of the crystal. Regime III crystallization results in an irregular fold surface where thickening would be very slow. On the other hand, regime I crystallization as in the case of linear polyethylene involves adjacent re-entry and a relatively more regular fold surface allowing faster lamellar thickening.

2.6   Copolymer Crystallization Theory

Having discussed the theories for crystallization in homopolymers, we now proceed to focus on the theories for random copolymers. The most relevant of these models are presented below. The merits and shortcomings of each theory are also pointed out to aid in the assessment of the soundness of their predictions. In all these treatments, a copolymer is considered as being comprised of two types of units - crystallizable A units, and B co-units. The latter represent the comonomers (or branches) in an actual copolymer. The presence of co-units gives rise to the possibility of these units being either completely rejected from a crystal lattice, or being uniformly included in the lattice. The former case, where the co-units serve to effectively section a copolymer into chains (or sequences) of different lengths, is termed as the *exclusion model*. The latter case, where the comonomers are uniformly included in the lattice formation, leading to a defective crystal structure, is named as the *uniform inclusion model*. These two extremes are depicted schematically in Figure 5.
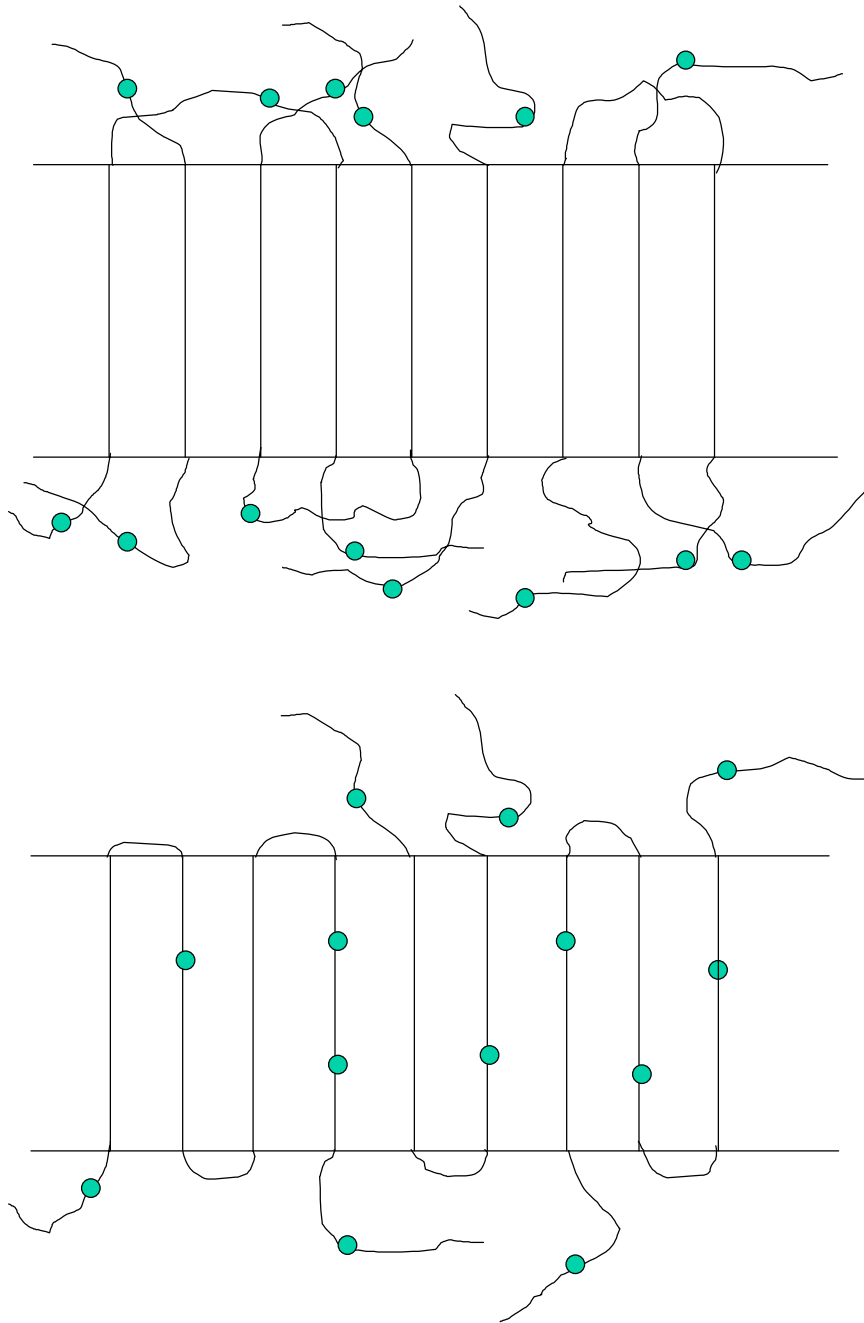
Figure 5 The exclusion (top) and uniform inclusion (bottom) models as the extreme
cases for crystalline random copolymers (Adopted from Ref. 40)

2.6.1   Flory's Theory of Copolymer Crystallization

In a theory modeling the crystallization of copolymers developed by Flory[25,35], the co-units are considered as defects that are completely excluded from the growing crystal. All sequences of a crystallite are composed only of A units, while the melt includes both A and B units. In other words, the presence of B units results in the partitioning of the polymer into sequences of A units of varying lengths that can aggregate in an ordered fashion to form a crystallite. However, there exists a limiting sequence length, ζ^*, of the crystallite that can be in equilibrium with the melt at a given temperature. Crystallites of sequence length below ζ^* will either not be formed at all or will vanish at equilibrium. The expression derived for ζ^* in this treatment is given by:

(8)
$$\varsigma^* = \left[\ln\left(\frac{DX_A}{p} \right) + 2\ln\left(\frac{1-p}{1-e^{-\theta}} \right) \right] \left[\frac{-1}{\theta + \ln p} \right]$$

where X_A = the mole fraction of crystallizable A units

$$D = \exp\left(\frac{-2\sigma_e}{RT} \right)$$

$$\theta = \left(\frac{\Delta H_u}{R} \right)\left(\frac{1}{T} - \frac{1}{T_m^0} \right)$$

Here, σ_e = the surface free energy per unit

ΔH_u = the heat of fusion per unit, and

T_m^0 = the melting temperature of the pure polymer.

The parameter, θ, is a measure of the undercooling, and D accounts for crystal surface free energy effects. The variable, p, is the sequence propagation probability of A units i.e., p is the probability that an A unit is succeeded by another A unit without being influenced by the nature of the preceding unit, in a sequence. This probability is related to the mole fraction of crystallizable units, X_A, as follows:

$$p = X_A \qquad \text{for a random copolymer}$$

$$p > X_A \qquad \text{for a block copolymer}$$

$$p < X_A \qquad \text{for an alternating copolymer}$$

The melting point depression (from that of a pure homopolymer) of the thickest possible crystals whose $\zeta^* \to \infty$ as predicted by this theory is given below.

$$(9) \qquad \frac{1}{T_m} - \frac{1}{T_m^0} = -\left(\frac{R}{\Delta H_u}\right) \ln p$$

These thick crystals are in equilibrium with a melt of overall composition, p. It is also implicit in Equation (9) that as the temperature decreases, the limiting sequence length also decreases, resulting in the formation of crystallites whose sequence length is smaller than $\zeta^*(T_m)$. Then the crystallinity at any temperature, T, is determined from the melt composition coexisting in equilibrium with crystallites of sequence length greater than $\zeta^*(T)$. The degree of crystallinity, w^c, is estimated as the sum of all sequences involved in the formation of crystallites and is given by the following expression:

$$(10) \qquad w^c = \sum_{\zeta^*}^{\infty} w_\zeta^c = \sum_{\zeta^*}^{\infty} \left(w_\zeta^0 - w_\zeta^e\right)$$

where w_ζ^0 = the weight fraction of ζ sequences of A units in the completely molten copolymer, and

w_ζ^e = the weight fraction of ζ sequences of A units in the melt in equilibrium with the crystallites.

The limiting sequence length, ζ^*, is obtained by letting $w_\zeta^0 = w_\zeta^e$. The summation in Equation (10) involves only sequences of length, $\zeta \geq \zeta^*$ because only those sequence lengths are allowed to participate in the formation of stable crystallites, as alluded to earlier. The crystallinities calculated using this equation are in general an overestimation of the actual values. This is due to the fact that the sequences derived from the melt in

order to form crystallites reduce the amount of amorphous fraction to a corresponding extent.[36] Such a reduction has not been taken into account in Equation (10). It has been pointed out by Crist[36] that a more accurate from of this equation may be written as follows:

$$ f_c = \sum_{n=n^*}^{\infty} \left[w_n^0 - (1 - f_c) w_n^e \right] $$

where f_c corresponds to w_c and n corresponds to ζ of Equation (10). However, the contribution of the factor, $(1-f_c)$, is significant only at appreciable values of crystallinity. At higher temperatures of crystallization, $(1-f_c) \cong 1$, rendering the correction factor insignificant.

Equation (9) predicts a decrease in melting temperature with increasing comonomer content, i.e., decreasing *p*. This prediction has been verified experimentally by numerous studies on a variety of copolymers, the details of some of which are discussed later. However, the melting point depression calculated using this expression is invariably smaller than that observed experimentally. This is a result of the condition that only sequences equal to or longer than ζ^* are allowed to participate in crystal formation. At temperatures very close to the temperature for incipient stability of crystallites, it is evident that ζ^* is very large. However, the total number of very long sequences is small and results in negligible values for the equilibrium crystallinity at this temperature. Therefore, the degree of crystallinity assumes a value very close to zero for a considerable temperature range below T_m, where it drops to zero. The observed melting temperature is not a sharp transition and that melting does not terminate abruptly at T_m as predicted by the theory. Another major discrepancy is that the heats of fusion calculated for a homopolymer from this analysis of copolymers are much lower than those measured experimentally by methods such as those of depression in melting point of the homopolymer by a diluent. This can also be deduced by examination of Equation (9), wherein the depression in melting point is shown to be inversely proportional to the heat of fusion, ΔH_f.

Flory's prediction of comonomer exclusion has been experimentally verified by a number of investigations including the one by Baker and Mandelkern.[37] The crystallization and fusion properties of a series of polymethylene copolymers with varying concentrations of methyl and *n*-propyl side groups were studied. A plot of the melting temperatures vs. branch concentrations of the copolymers was made to examine the nature of comonomer inclusion/exclusion from the crystal. The data obtained experimentally were compared to the case where the crystal lattice remains pure. Perfect agreement was achieved for the copolymers with *n*-propyl side groups while remarkable differences were seen for the copolymers with methyl branches. This observation implies that the methyl groups must be present in the crystal lattice as an equilibrium requirement (the authors have suggested a possible solid solution or compound formation), while the *n*-propyl side groups are excluded from the crystal lattice. This result is also in agreement with that of Flory and Richardson[38] from their study on ethylene copolymers.

So far, we have discussed the postulates of Flory's theory of crystallization of copolymers. It provides a very rigorous treatment of the processes of melting and crystallization in copolymers, and some of its predictions are verified experimentally. However, the equilibrium conditions for these processes as outlined by the theory are never realized in reality for copolymers. The main reasons being,

1. the kinetic restrictions imposed on chain transport to the surface of a crystallite by the presence of branches, and
2. the fact that the longest sequences in these copolymers crystallize by chain folding (and not as an extended chain crystal) and that large undercoolings are necessary.

These factors contribute to a greater extent with increasing comonomer content resulting in larger deviations from the predictions of the theory.

2.6.2 Sanchez and Eby's Model for Copolymer Crystallization

Sanchez and Eby[39,40] have proposed an alternative approach to the crystallization of copolymers that accounts for the kinetic nature of the processes involved. As in Flory's theory, a copolymer comprised of crystallizable A units and B co-units is adopted in this model. The two extreme cases of the crystalline state, namely those of comonomer exclusion and uniform inclusion are also considered. An expression for the free energy of crystallization of the copolymer, ΔG, is derived based on the condition that "a real copolymer crystal is formed under kinetic conditions which determine the actual concentration of B co-units in the crystal"[39], and is given below:

$$
(11) \qquad \Delta G = \Delta G^0 - RT\left\{\frac{\varepsilon X_c}{RT} + (1 - X_c)\ln\left[\frac{1 - X_c}{1 - X}\right] + X_c \ln\left[\frac{X_c}{X}\right]\right\}
$$

where ΔG^0 = the free energy of crystallization of the homopolymer

ε = the excess free energy of a defect (due to the presence of a B co-unit) in the crystal lattice

X_c = the concentration of co-units in the crystal, and

X = the overall composition of co-units in the copolymer.

Then, the two extreme cases of comonomer distribution discussed above are represented by:

$$X_c \Rightarrow 0;\ \varepsilon \Rightarrow 0 \qquad \text{Exclusion Model}$$

$$X_c \Rightarrow X;\ \varepsilon \Rightarrow \infty \qquad \text{Uniform Inclusion Model}$$

The equilibrium concentration of the co-unit, X_{eq}, is expressed as:

$$
(12) \qquad X_{eq} = \frac{Xe^{-\varepsilon/RT}}{\left(1 - X + Xe^{-\varepsilon/RT}\right)}
$$

The departure of the crystallization process from equilibrium at any temperature can be determined by a combination of Equations (11) and (12). Furthermore, letting $\Delta G = 0$ for equilibrium and using the relationship,

$$\Delta G^0 = \Delta H_f^0\left(1 - \frac{T}{T_m^0}\right)$$

Equation (11) can be re-written as:

$$(13) \qquad \frac{1}{T_m^0} - \frac{1}{T_m} = -\frac{R}{\Delta H_f^0}\left\{\frac{\varepsilon X_c}{RT_m} + (1 - X_c)\ln\left[\frac{1 - X_c}{1 - X}\right] + X_c \ln\left[\frac{X_c}{X}\right]\right\}$$

where ΔH_f^0 = the heat of fusion of the homopolymer, and

$\quad T_m^0$ = the equilibrium melting temperature of the homopolymer.

This expression represents the melting point depression for the copolymer with respect to the homopolymer. For the case of uniform inclusion, $X_c \Rightarrow X$ and Equation (13) reduces to:

$$(14) \qquad T_m = T_m^0\left(1 - \frac{\varepsilon R}{\Delta H_f^0}X\right)$$

while for complete rejection of comonomer from the crystal lattice, $X_c \Rightarrow 0$ yielding the relationship,

$$(15) \qquad \frac{1}{T_m} = \frac{1}{T_m^0} + \frac{R}{\Delta H_f}\ln\left(\frac{1}{1 - X}\right)$$

Thus, the melting temperature depression in the case of co-unit inclusion (Equation (14) is principally an enthalpic effect due to the presence of defects in the crystal lattice. On the other hand, the depression for the rejection case (Equation (15) describes the entropic

effect arising from the necessity for sequential ordering of the chains during crystallization. Such a distinction, accounting for the kinetic effects and constraints to chain transport during crystallization of copolymers is a marked improvement over the postulates of Flory's theory.

Sanchez and Eby[39,40] have also demonstrated that the observed lamellar thickness at a selected crystallization temperature increases linearly with decreasing comonomer content. This result was based on the assumption that the fold surface free energy and the thickening at that temperature are independent of comonomer content. It is interesting to note that the same prediction has been made in Flory's equilibrium theory based on exclusion of co-units as well. Thus, it may be seen that similar predictions can be made from Flory's equilibrium theory as well as from Sanchez and Eby's kinetic theory. The choice of the treatment to be adopted to most appropriately model the crystallization behavior of a given copolymer must be based on experimental considerations. One such method involves the estimation of ratios between the observed heat of fusion from thermal analysis and the degree of crystallinity from X-ray diffraction studies ($\Delta H_f^*/x_c$). For the exclusion model, this ratio is independent of comonomer content as shown below.

$$(16) \qquad \frac{\Delta H_f^*}{x_c} = \Delta H_f^\infty - \frac{2\Delta H_e}{l}$$

However, for the case of uniform inclusion, a linear dependence on comonomer concentration, X, is obtained as indicated in the following equation.

$$(17) \qquad \frac{\Delta H_f^*}{x_c} = \Delta H_f^\infty - X\Delta H_d - \frac{2\Delta H_e}{l}$$

In the above expressions, ΔH_f^∞ = the heat of fusion of the pure homopolymer, ΔH_d = the defect heat of fusion, ΔH_e = the excess heat of fusion of forming the basal surfaces of a lamellar crystal and l = the lamellar thickness.

2.6.3   Other Copolymer Crystallization Theories

In addition to the two theories of copolymer crystallization discussed above, a number of other treatments are available in the literature. Among those are the model introduced by Pakula[41,42] where the two extreme cases of "non-effective and effective arrangement of segments in crystalline lamellae" are considered. This model provides a convenient means of comparing the predictions with experimental data since it correlates two independently measurable morphological parameters, namely crystallinity and long spacing.[41] Although it recognizes the kinetic effects arising from the strong hindrances imposed due to segmental diffusion in copolymers, it is plagued by the non-realistic assumption that all chain sequences longer than the critical length will contribute to the crystalline phase. The deviations from this assumption are particularly large at higher temperatures (closer to the melting temperature), when the critical length increases and the fraction of chains with such lengths becomes exceedingly small.

Wang and Woodward[43, 44] have provided a simple treatment of the crystallization in copolymers from solution. Their calculations yield values for the number of monomer units per fold, and per crystal traverse, and also provide their variation with crystallization temperature. However, this treatment fails to address the concepts of equilibrium and the process of melting in copolymers.

Helfand and Lauritzen[45] have also developed a theory for the crystallization of copolymers. This theory is based mainly on the kinetic theory for polymer crystallization due to Lauritzen, DiMarzio and Passaglia.[46] In addition, Helfand and Lauritzen's theory recognizes the free energy costs of incorporating a comonomer unit in the crystal lattice. They rightly point out that the inclusion of co-units not only "modifies the thermodynamic properties, but also profoundly affects the kinetic barriers to crystal growth". A detailed description is available in Ref. 45. However, the major predictions from their theory are summarized below:

1. The concentration of comonomer incorporated into the copolymer crystal is higher than that predicted by the equilibrium theory. As a result, the melting temperatures of the crystals are lower than those predicted.

2. Conditions that speed up the growth process will increase the extent of co-unit inclusion. For instance, decreasing temperature increases the inclusion of co-units.

3. The lamellar thickness of the copolymer is larger than that of a pure homopolymer, at the same crystallization temperature. The extra thickness compensates for the free energy costs of incorporating co-units in the crystal.

Thus, this theory not only considers the kinetic factors involved in the crystallization of copolymers, but also accounts for the effects of the different states of a growing substrate on the growth rate of the crystals. Furthermore, the conclusions from this theory are consistent with those from the model proposed by Sanchez and Eby[39] for the crystallization of copolymers.

2.7   Theoretical Considerations for Homo- and Copolymer Crystallization

The theories developed for modeling the crystal forming processes in homo- and copolymers were reviewed in the above two sections. It was also pointed out that some of the assumptions made were non-realistic, rendering a given theory less useful for modeling the actual crystallization process. Now we proceed to analyze the applicability of some of the equations and approximations derived above in appropriately representing the experimental results.

It was mentioned in Section 2.5.2 that the Gibbs-Thomson equation (Equation (6) is a very general expression applicable to a wide variety of materials. Accordingly, this relationship has been used by several investigators to estimate values of crystal thickness distributions from the endotherms obtained via Differential Scanning Calorimetry (DSC).[47,48,49,50,51] It has been demonstrated[52] for linear polyethylene (LPE) that the calculated crystal thickness distributions from the Gibbs-Thomson equation can be matched to those obtained experimentally (via Electron Microscopy and Longitudinal Acoustic Mode Raman Spectroscopy) using appropriate values of the fold surface free energy, σ_e. It must however be remembered that heating rate plays a significant role

since rates greater than 10°C/min. could give rise to superheating effects. Furthermore, larger deviations are expected at melting temperatures closer to T_m^0 due to the temperature sensitivity of the Gibbs-Thomson equation in this temperature range. Even small changes in T_m lead to large variations in the calculated thickness distributions. Above all, additional corrections are necessary to account for the heat transfer to the sample and the breadth of the melting process.

The same analysis has been extended to copolymers to investigate the effects of comonomers on the crystal thickness distributions.[52] It was shown in an earlier discussion on Flory's copolymer theory[25,26] that random copolymers melt over a much broader range of temperatures compared to LPE owing to the presence of a wide distribution of chain lengths.[53] As a result, their equilibrium melting temperatures are not easily measured by experimental techniques and are estimated from Flory's theory. The distributions derived from Gibbs-Thomson equation for the copolymers do not match those obtained experimentally. The values of T_m^0 and σ_e that are required to force a close match are unreasonably low. Even attempts to attain better fits by varying the heating rates failed because identical distributions with only very minor changes were obtained at different heating rates.[52] This complete failure of the applicability of the Gibbs-Thomson equation to the melting of copolymers is a direct result of the sequence distribution in such materials. The distribution of crystallizable chain lengths varies as a function of temperature during the melting process. This in turn influences (changes) the free energy and chemical potential associated with the melt.[35,54] However, the derivation of the Gibbs-Thomson expression is based on the condition that the melt composition is constant. Thus, it is seen that the nature of the fusion process in copolymers imposes restrictions on the use of the Gibbs-Thomson equation to determine crystal thickness distributions in copolymers, while the same calculation can be achieved with greater success in linear polyethylene.

A few other aspects of the fusion and crystallization processes in copolymers deserve special attention. It may be recalled that only sequences of length greater than a critical length, ζ^*, can form crystals in copolymers. The value of ζ^* increases with increasing temperature until it tends towards infinite values. Then, the equilibrium melting temperature, T_m^e, represents the melting of the thickest possible crystals. The

formation of such infinitely thick crystals is highly unlikely in copolymers mainly due to the kinetic restrictions imposed on chain transport. It has been pointed out by Crist and Howard[36] that the number of such crystals is so small that this melting transition is almost impossible to measure. Both the peak melting temperature (T_m^P) and the final melting temperature (T_m^f) estimated from the melting traces fall well below the equilibrium melting temperature. These authors also estimated the probability density function, -$df_c/d\zeta^*$ for the weight fraction of crystals with thickness ζ^*. The distribution obtained on plotting this probability density function vs. the thickness ζ^* is shown in Figure 6. It is clearly seen that ζ^* increases more rapidly at higher temperatures and that the peak melting temperature is in no way related to the most populated crystal thickness (centered at $\zeta^* = 25$ in the figure). It is also indicated that the breadth of the melting process in copolymers (due to the different lengths, ζ^*) is primarily responsible for the inability to determine crystal thickness distributions from the melting curves.

It is also important to recognize the nature of the primary crystallization in the copolymers. This process bears a significant influence on the nature of the secondary crystallization as well as on the morphology developed in the material. The idea of a critical sequence length, ζ^*, discussed in the previous paragraph implies that a significant degree of undercooling must be achieved for the crystallization of ethylene sequences in a copolymer (since ζ^* decreases with temperature). The primary crystallization from such an undercooled melt involves crystallization of sequences regardless of their lengths, provided they are longer than a certain critical length determined by the temperature. The longest sequences crystallize by forming chain-folded crystals. Such a primary process pins down the remaining chains and restricts their mobility and transport. This in turn hinders further crystallization during cooling. Furthermore, the differences in times afforded by variations in cooling rates are not sufficient to give rise to considerable differences in the degrees of crystallinity. A direct implication of this fact is the experimentally observed insensitivity of the crystallinity and long periods of copolymers to the cooling rates employed.[36,55]
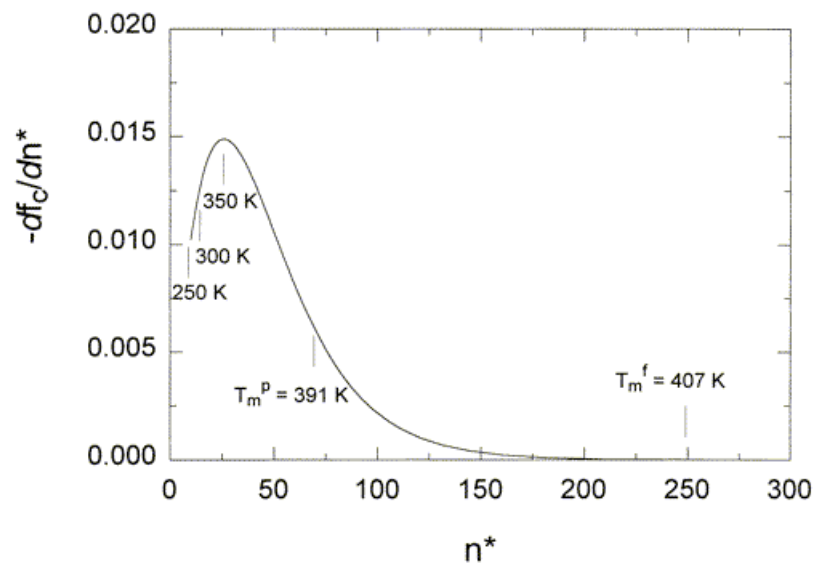
Figure 6 Equilibrium distribution of crystalline sequences in a random ethylene/1-butene copolymer (Adopted from Ref. 36).

Thus, the hampering of segmental mobility by the primary stage of the crystallization process in copolymers leads to conditions far removed from the predictions of Flory's equilibrium theory, and strongly influences the secondary crystallization process. An understanding of the nature of the secondary crystallization process and its impact on the time-dependent properties in such copolymers is the primary goal of the present investigation.

2.8   Nature of the Copolymers

The above section was focused on the theories proposed for the crystallization behavior of random copolymers. It is also essential to understand the nature of the copolymers used in the current study and recognize the specific features that differentiate them from the remaining "polyethylenes". A brief review of the historical evolution of the different types of low density polyethylenes starting from the discovery of Ziegler-Natta type catalyst systems to that of the metallocene-based ones is presented in this section. The metallocene-based ethylene/α-olefin copolymers used in the present study are also compared with the other existing types of polyethylenes such as Low Density Polyethylene (LDPE), Linear Low Density Polyethylene (LLDPE), Ziegler-Natta based systems etc., with specific reference to the features that make them ideal for the present investigation.

2.8.1   Ziegler-Natta Based Copolymers

The search for newer methods to synthesize polymeric materials, in particular polyethylene, with exceptionally controlled molecular structure and desired properties has been ongoing for several decades. A major breakthrough in this area occurred with the discovery in 1953 by Ziegler and his co-workers[56] that a combination of transition metal halides with alkylaluminums in an inert hydrocarbon could catalyze the polymerization of ethylene to produce highly linear and high molecular weight polymer.

Several transition metal compounds such as those of nickel, zirconium, titanium, etc. were utilized and were found to give similar results, with titanium being the most active. The commercial significance of this discovery was the fact that these polymerizations could be carried out under highly moderate conditions of temperature and pressure compared to the previously employed procedures. In an independent and concurrent investigation, Natta and co-workers[57,58] established that the above catalyst system could also polymerize propylene to yield a polymer with a high degree of isotactic stereoregularity. They also extended their study to the polymerization of α-alkenes and successfully employed transition metal compounds in their lower valence states than those used by Ziegler *et al.*[56] Independent research was carried out in several industrial laboratories in the United States at the same time. These investigations led to the discovery of a related class of silica-supported chromium trioxide catalysts by the Phillips Petroleum Company[59,60] during the early 1950's. These catalysts constituted some of the earliest low-pressure catalyst systems for the production of linear high density polyethylene.

These discoveries introduced a new class of catalysts as well as of polymers. They also enabled achieving a high degree of control in the synthesis of some of the most readily available and cheap monomers such as ethylene and propylene. In the case of ethylene, it had become possible to produce a more linear and high molecular weight polyethylene. Whereas in the case of propylene, it had become possible to synthesize linear and highly stereoregular molecules by exercising control on the propagation step. In recognition of the profound effect that these discoveries had on the field of synthetic polymer chemistry, Ziegler and Natta were awarded the Nobel Prize for Chemistry in 1963, and the catalyst system was appropriately named after them.

2.8.1.1   Linear Low Density Polyethylenes (LLDPE)

This class of polymers are formed by the copolymerization of ethylene and α-alkene comonomers in the presence of Ziegler-Natta catalysts, resulting in side chains at the point of insertion of the alkene.[61,62] The structure of these copolymers can be

carefully manipulated by varying the manufacturing conditions according to the application desired. The branches in LLDPE not only lower the degree of crystallinity compared to High Density Polyethylene (HDPE) but also lower the density of the material (similar to Low Density Polyethylene-LDPE). However, LLDPE is superior to LDPE with respect to ease of processability, impact, tensile and tear strength as well as optical properties. Furthermore, LDPE consists of short chain as well as long chain branches that disrupt the crystal structure and affect desirable properties such as melt strength. LLDPE, on the other hand, is comprised only of branches of a constant length leading to potentially higher crystallinity and higher rigidity compared to a similar LDPE. These factors have contributed to the immense success of LLDPE over typical low density polyethylenes in the recent years.

2.8.2   Metallocene Based Copolymers

Several studies were carried out with the aim of understanding the polymerization mechanism using Ziegler-Natta catalysts. These studies led to the hypothesis that the "propagation step involved the insertion of an activated monoalkene molecule into a transition metal-carbon bond"[63] and that the high degree of "isotactic stereocontrol was associated with the chiral structure of the transition metal complex".[64] These observations on the heterogeneous Ziegler-Natta catalyst systems suggested that it may be possible to carry out similar polymerizations using homogeneous transition metal organometallic derivatives if the active complex can be formed. Several attempts at finding such a soluble catalyst were made, culminating in the discovery in the early 1980's by Kaminsky and coworkers[65] that metallocene complexes of transition metals, when activated with alkylalumoxanes, yielded highly active and soluble catalysts with similar catalytic activity as the heterogeneous Ziegler-Natta catalysts. The discovery of metallocene-based catalysts provided an alternative to the heterogeneous system of catalysts in general. In particular, it had become possible to synthesize isotactic, high molecular weight polypropylene (which was not feasible before the use of alkylalumoxanes).

The first commercial copolymers based on the metallocene-based catalysts were produced by Exxon in 1991 using an achiral single-site catalyst.[66] In 1993, Dow Chemical began production of copolymers using a cyclopentadienyl amide titanium catalyst, whose structure is represented in Figure 7. The term "Constrained Geometry Catalysts" is derived from the open and highly reactive nature of the metal (here Ti) atom resulting from the presence of a short dialkylsilyl bridging moiety.

2.8.2.1   Metallocene-Based Ethylene/α-Olefin Copolymers

This class of materials owes it origin to the recent developments in metallocene-based catalyst chemistry and has spurred renewed interest in the effect of comonomer distribution on the morphology and physical properties of a polymer. These copolymers possess all the favorable characteristics of LLDPE's in addition to a high degree of control over the stereospecificity and the molecular weight distribution of the resulting materials. The single-site catalysts involved in the synthesis of such copolymers permit a uniform distribution of comonomers in the various polymer chains,[67] i.e., the distributions of comonomers in the different polymer chains are identical to each other, irrespective of chain length. This is in sharp contrast to the Ziegler-Natta based systems that yield a broad distribution of comonomers among the various polymer chains. Both the metallocene as well as the cyclopentadienyl amide catalysts result in random incorporation of ethylene and α-olefins without the use of excess comonomer. Furthermore, the randomness is achieved independent of chain length. It must however be noted that the cyclopentadienyl amide type catalysts yield copolymers with long chain branching as well. The metallocene-based copolymers may include a variety of branches such as ethyl, butyl, pentyl, hexyl etc. Copolymers made by Dow Chemical using the single-site constrained geometry catalyst technology (CGCT) are employed in the present study.
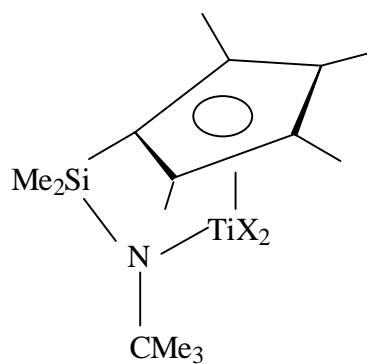
Figure 7 Structure of cyclopentadienyl amide titanium catalyst used in the synthesis of ethylene/α-olefin copolymers (Adopted from Ref. 66).

2.9   Literature Review

This section is a review of some of the existing literature relevant to the present study on ethylene/α-olefin copolymers. A wide variety of aspects including structure, morphology, crystallinity, crystallization and melting behavior, etc. of the copolymers are covered by a large number of investigations. In order to gain the most information from these studies, this section is divided into several sub-sections related to the above-mentioned aspects. Furthermore, wherever possible, the behaviors of copolymers are compared to those of the corresponding homopolymers.

2.9.1   Comonomer Exclusion

It may be recalled from the copolymer crystallization theories outlined in Section 2.6 that the co-units present in a copolymer may either be completely rejected from the crystal (exclusion) or uniformly included as an equilibrium requirement (inclusion). Flory's theory[25,35] is based on the exclusion model, while Eby and Sanchez[39,40] have considered both the possibilities. The following is a brief survey of some of the investigations that clarify the nature of comonomer inclusion/exclusion in random copolymers.

Baker and Mandelkern[37] have examined the crystallization and fusion properties of a series of polymethylene copolymers with varying concentrations of methyl and *n*-propyl side groups. The measured melting temperatures were plotted as a function of branch concentrations of the copolymers and compared to the case where the crystal lattice remains pure. Perfect agreement was achieved for the copolymers with *n*-propyl side groups suggesting that they are excluded from the crystal lattice. However, remarkable differences observed for the methyl branch-containing copolymers implied that these branches must be present in the crystal as an equilibrium requirement. This result is also in agreement with that of Flory and Richardson[38] from their study on methylene copolymers.

Alamo *et al*.[68] have studied a variety of copolymers including fractions of ethylene/1-butene, ethylene/1-octene, ethylene/vinyl acetate, ethylene/propylene, hydrogenated polybutadienes and diazoalkane copolymers with the aim of understanding the influence (if any) of the chemical nature of the comonomer on the structural and thermodynamic properties of the copolymer. The melting temperatures obtained via dilatometry revealed that all copolymers except those containing the methyl side groups could be represented by a single curve on the T_m vs. comonomer content plot. The methyl group containing copolymers displayed higher T_m's suggesting that these groups enter the crystal lattice on an equilibrium basis. However, the T_m's of the fractions of the ethylene/1-butene copolymers from DSC showed deviations from such a single curve. It was argued that these deviations must be due to differences in sequence distributions rather than due to differences in nature of the side groups. This argument was based on the fact that the hydrogenated polybutadienes (that also contain ethyl branches) fell on the same curve. The above results are also concordant with those of Flory and Richardson[38] and imply that the melting temperatures are independent of the chemical type of the co-unit (except methyl), provided the sequences are randomly distributed in the copolymer.

As a follow-up investigation, the same authors carried out a similar study[69] on a series of ethylene/1-butene random-type copolymers synthesized using the method of Kaminsky *et al*[70]. These materials were characterized by a most probable molecular weight distribution in addition to a narrow composition distribution. As a result, the need for fractionation of the starting material was eliminated and there were no further ambiguities regarding the randomness of sequence distribution. The melting temperatures of these copolymers were obtained via DSC measurements and compared to the results of the wide range of copolymers from the previous study.[68] The two sets of data were coincident on each other, clearly indicating that the results are independent of the chemical nature of the side group. Furthermore, it provided verification of the argument posed earlier for the deviation observed for the ethylene/1-butene copolymer fractions from the rest of the data. In other words, it confirmed that the differences observed from the single curve in the previous study were due to differences in sequence distribution, and not due to the chemical nature of the comonomer. Additional support

for this confirmation is derived from the results of Clas *et al.*[71], who have obtained the melting temperatures (T_m) for a series of ethylene/1-octene and ethylene/1-butene copolymers. Although no dependence of the melting points on the comonomer type was noted, their values are significantly higher than those reported for copolymers with a completely random sequence distribution.

Alamo and Mandelkern[72] have reported similar results from their study on random ethylene/α-olefin copolymers. They noted that it was possible to represent different types of branches by a single curve on the melting temperature vs. molecular weight plots.

Flory's prediction that all branches longer than methyl are excluded from the crystal lattice has also been confirmed by means of ^{13}C NMR and selective oxidation techniques.[72] For copolymers containing ethyl and longer groups, the spin lattice relaxation times from ^{13}C NMR are very short suggesting that these branches are concentrated in a single mobile and disordered phase. In the chemical oxidation study, the ethyl branch content dropped to an experimentally negligible value of 0.08% with the loss of ~ 60 % of the sample in only 6 hours of oxidation. Thus the branches are easily accessible to the oxidizing agent, while the crystalline core is not. This further implies that the ethyl branches are located in the disordered amorphous phase rather than in the crystalline phase. These observations are consistent with other similar investigations[73,74,75] via ^{13}C NMR and chemical oxidation on high-pressure free radical polymerized long chain polyethylene. It was concluded that ethyl and butyl side chains were predominantly excluded from the crystal lattice.

The rejection of co-units from the crystal lattice and their subsequent accumulation at the surface of the crystallites have led some authors to believe in the existence of an interfacial region.[72] These authors have reported the presence of a significant interfacial region of thickness ~20 - 40Å in random copolymers. The thickness of this region was found to increase with increasing comonomer content, while it remained invariant with molar masses up to 100,000 g/mol. The observed invariance of the interfacial thickness with molecular weight for the copolymers was vastly different from the corresponding increase reported for homopolymers.[76,77] In contrast to the invariance of the other parameters examined on the nature of comonomer, the interfacial

thickness of the copolymer was found to be slightly larger for the longer hexyl branches. This result cannot however be generalized to the conclusion that interfacial thickness increases with increasing size of the comonomer. It must be noted that the validity of the presence of such an interfacial region is highly questionable, and any related results must be viewed with caution. More favorable explanations for the nature of the regions comprising the rejected branches on the surface of crystallites may be proposed.

2.9.2   Morphology

2.9.2.1   Dual Morphology - Lamellae and Bundles Crystals

The different models for the chain folding process in semicrystalline polymers were discussed in Section 2.1. It may be recalled that both Keller's and Flory's models require that (at least) some of the chains must return to the face of the crystallite from which they depart. For a copolymer with a non-crystallizable co-unit, it is fairly unlikely that a chain re-entering a crystallite after traversing through it will be devoid of the co-units.[10] This situation leads to additional congestion in the interfacial area (not in the sense of Mandelkern's[72] "interface"!) due to the presence of chain sequences from different crystallites. As a result, the presence of comonomers suppresses the crystal growth in one or more lateral directions and thereby the lamellar morphology characteristic of homopolymers. The extent of this suppression increases with increasing comonomer content in the copolymer. Then it is possible that in more highly branched copolymers, the chains can dissipate their spatial constraints, while still satisfying the spatial requirements, by simply aggregating into bundles of chains.[78,79] Such an aggregation minimizes the demands on the cooperativity requirements of these disordered and constrained chain sequences. Therefore, the morphology in more branched copolymers may involve an aggregated bundle structure ("fringed-micelle"-like crystals), in addition to the chain folded array expected for the longest sequences. This conclusion is highly relevant to the current study on copolymers of varying branch contents. It will

be shown by means of calorimetric, infrared and microscopic techniques that such a change in morphology does actually occur with varying comonomer content.

A dual morphology such as that discussed above has been observed in several investigations on ethylene copolymers. One example is the study by Mathot *et al.*[80] of the effects of comonomer content on the crystallization and melting behavior, as well as on the morphology of both homogeneous and heterogeneous ethylene copolymers. The results obtained from Transmission Electron Microscopy (TEM) indicate the presence of two very different types of crystal morphologies, namely lamellar and granular. In a copolymer containing ~ 11 % 1-octene, a matrix of lamellae with thickness ~ 9 nm as well as additional granular structures were observed. However, on moving to a copolymer with ~ 18 % comonomer content, the lamellae were lost. The morphology in this case seemed to be dominated by granular structures of ~ 6-12 nm in dimension.

Deblieck and Mathot[81] have made similar observations on ethylene/1-octene copolymers by means of Scanning Electron (SEM) and Transmission Electron Microscopies (TEM). The samples were examined after removing non-crystallizable and low crystallinity material using solvent extractions. The micrographs collected clearly indicate that these materials are comprised of distinct regions of highly different crystallinities - lamellae 0.5 to 1 μm long and 13 to 14nm thick, short lamellae 0.05 μm long and 4 nm thick, and compact semicrystalline domains (CSDs) made up of nodular entities that are radially interconnected by means of thick and long lamellae. The morphology observed was found to vary significantly with comonomer content. For instance, when the 1-octene content increases from 5.7 to 8.5 mole %, regions of low crystallinity (compared to the relatively more crystalline lamellar regions) change from being dispersed to being continuous with the complementary phase.

Mirabella *et al.*[82] have carried out a similar investigation on a series of ethylene copolymers after removal of low crystallinity material. The transmission electron micrographs revealed the presence of large voids in the place of the etchable removed material, in contrast to those for HDPE and LDPE. The average particle diameters of the removed phase was estimated to be ~ 0.2μm. This dimension falls in the range of particles that are ideal for toughening of brittle plastics[83], which helps to explain the extremely high fracture toughness (29kJ/m^2) observed in these materials. The authors

concluded that the copolymers are comprised of a significantly broad spectrum of species ranging from very low crystallinity to those similar to HDPE. Furthermore, the low crystallinity, highly branched material could be pictured as being embedded in a continuous semicrystalline matrix of highly crystalline material. Then, this rubbery embedded phase can enhance the toughness of the material similar to the rubber-like phase in high impact polymers such as styrene, ABS, nylon etc.

As discussed in Section 2.8.2, the advent of newer technology in the past decade[84] has made it possible to synthesize homogeneous ethylene copolymers with very narrow molecular weight distributions and lower crystallinities than the Linear Low Density Polyethylenes (LLDPE) that are heterogeneous in nature. Such copolymers made using the INSITE® constrained geometry catalyst technology (CGCT) are the focus of the present study. These copolymers present a broad range of physical and morphological features that have spurred increasing interest in this area, and have become the topic of several investigations over the last few years. One such study is the detailed examination of the thermal and morphological behavior of a series of ethylene/1-octene and a few ethylene/1-butene and ethylene/propylene copolymers, via DSC and TEM by Minick *et al*.[85] The transmission electron micrographs for an ethylene/1-octene copolymer with ~ 38 branches per 1000 carbon atoms reveal a granular texture, with the granules aligned in beaded strings of thickness between 100 and 130Å, without any lamellae. The boundaries between the stained amorphous and unstained crystalline regions were very diffuse. The authors have suggested that such an organization of polymer chains resembles the fringed micelle concept. When the number of branches was decreased to 25 per 1000 carbons, the beaded strings (which are now only 75-100 Å thick) were seen to be aligned in large clusters providing directionality to the morphology.

The effect of thermal history was observed via a comparison of two samples - one that was quenched and another slowly cooled. The slowly cooled sample possessed some long and curved lamellae that are ~ 140 Å thick with a few beaded strings and granules interspersed in the spaces in between. The edges between these lamellae and the adjacent stained regions were well defined, indicating better surface order and a "possibility of chain folding".

The influence of comonomer type was also investigated by comparing an ethylene/1-octene and an ethylene/1-butene copolymer with similar molecular weights and densities.[85] The two copolymers did not display significant differences in behavior except for the fact that a higher percent of 1-butene comonomer was required than 1-octene to yield a copolymer with a given density. This in turn decreases the number of crystallizable ethylene sequences that are capable of forming lamellar crystals. Furthermore, rough estimates of σ_e were obtained based on the crystal thicknesses, L, from the micrographs. These values increase with increasing comonomer content (indicating less regular folding in the crystal structures) and are much higher than those reported for regular chain folded crystals[86] ($\sim 100 \text{ergs/cm}^2$) while being much closer to those reported for bundled crystals[87,88] ($\sim 300 \text{ergs/cm}^2$). These results further suggest that as the comonomer content increases, the number of ethylene sequences long enough to form chain-folded lamellae decrease; and that even the chain folded crystals encountered in such copolymers do not possess very high degrees of regular chain folding.

Based on the results obtained, the authors[85] have classified such copolymers into four types, according to their densities and morphologies. Type I constitutes copolymers with densities less than 0.89 g/ml that do not exhibit any lamellar morphology, but are dominated by the bundled crystals that also give rise to the low degrees of crystallinities in these materials. Type II comprises copolymers with densities between 0.91 and 0.89 g/ml. These possess a mixed morphology including both the lamellae and bundled crystals. Copolymers whose densities are between 0.91 and 0.93 g/ml fall under Type III and predominantly exhibit thin lamellae and small spherulites, whose sizes are a function of the comonomer content. Type IV constitutes copolymers with densities larger than 0.93 g/ml and exhibits a lamellar morphology with well-developed spherulites as seen in High Density Polyethylene. This classification is schematically represented in Figure 8. Although this classification is not a strict representation of the morphological features of such copolymers, it may be taken as the basis for further investigations in this area.
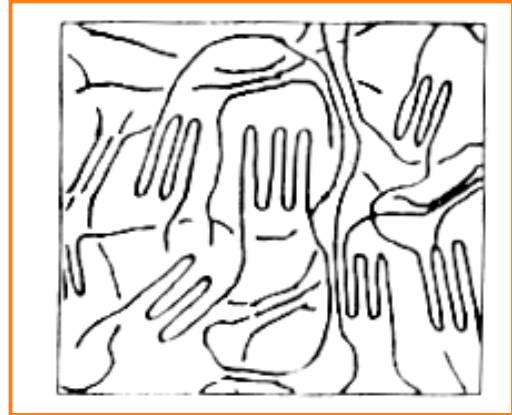
TYPE I

Fringed Micelles
No lamellae
No Spherulites
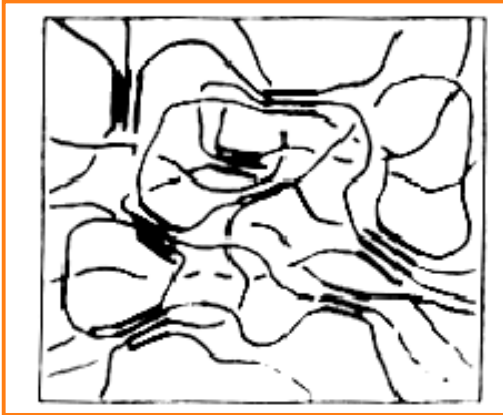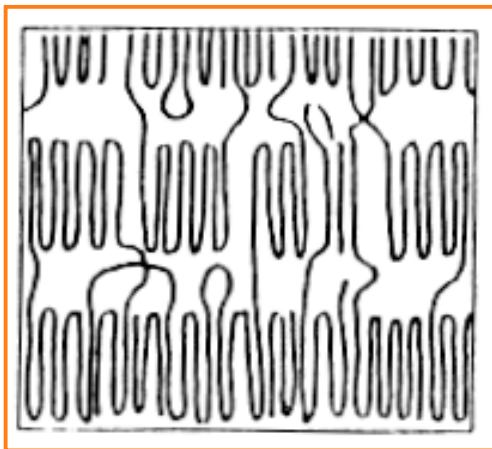

TYPE II

Fringed Micelles
Lamellae
Spherulites

TYPE III

No Fringed Micelles
Lamellae
Spherulites

TYPE IV

No Fringed Micelles
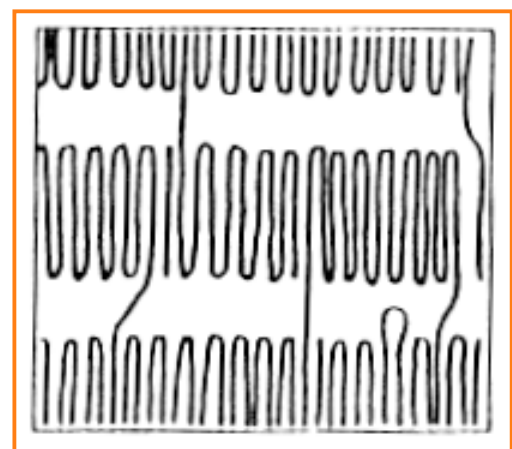Lamellae
Spherulites

Figure 8 Classification of copolymer morphology (Adopted from Ref. 85)

2.9.2.2   Nature of Spherulites in Copolymers

Peeters *et al.*[89] have examined the nature of spherulites formed in a series of ethylene/1-octene copolymers. Since the branches are completely excluded from the crystals, it is possible that the growth of a crystal face can be halted before being completed, when a branch is encountered. Thus, the branches impede crystal growth and favor multiple nucleation at a given crystal surface. Therefore, such copolymers crystallize either under Regimes II or III, which favors spherulitic growth. A further increase in comonomer content increases the difficulty of the chains to participate in nucleation and destroys any organized supermolecular structure. These expectations are verified by the results of both Optical Microscopy and Small Angle Light Scattering, where a spherulitic structure is observed for the moderately branched copolymers, and no specific morphological features can be recognized for the highly branched ones (> 25 mole % branches). In the former case, the size of the spherulites decreases with increasing branch content and increasing cooling rate, as expected. For copolymers with intermediate branch contents, it is more likely that small sheaves are formed, instead of completely formed spherulites.

It has been reported by Mandelkern and Maxfield[90] that the supermolecular structure developed on quenching branched polyethylenes from the melt is strongly dependent on the branching concentration and molecular weight distribution. In contrast, isothermal crystallization at higher temperatures followed by cooling to room temperature always yielded a spherulitic structure. This study was later extended to broader crystallization ranges and polydispersities, with the aim of separating the influence of various parameters on the morphology developed.[91] It was shown by means of Small Angle Light Scattering (SALS) and a combination of microscopy techniques that a diverse set of supermolecular structures are developed in a given material under conditions of non-isothermal crystallization from the melt. These morphological structures are designated as follows, based on their appearance in the SALS patterns: Types a-c are four-fold symmetric and yield spherulites of progressively deteriorating order; type d that exhibits an azimuthal dependence of scattering is indicative of rod-like aggregates of lamellae; type h that displays no angular dependence is due to randomly oriented lamellae, and: type g that is similar to type h and is due to rod-like structures that

have breadths comparable to their lengths. It was noted that there exists a restricted domain of molecular weights and quenching temperatures that can yield spherulitic structures. This range narrows with increasing molecular weight and branching concentration. Eventually, a molecular weight and/or branch content is reached beyond which spherulites cannot be formed. Within the domain of spherulite formation, more ordered superstructures result from lower molecular weights and higher crystallization temperatures.

It will be shown in the next section that comonomer content, crystallization conditions and molar mass play a major role in determining the thermodynamic properties (such as melting temperature, enthalpy of fusion and degree of crystallinity) of copolymers. The same parameters also influence the morphology developed in the material. The correlation between the thermodynamic properties and the superstructure developed in branched polyethylene has been examined in detail by Mandelkern and Maxfield.[90] It was shown that the thermodynamic properties are independent of the morphology involved. In other words, a variety of supermolecular structures may be obtained on quenching the samples to different temperatures. However, the thermodynamic properties measured at the various quenching temperatures are continuous over the entire crystallization range and the different morphological forms. For instance, for a sample with 7 mole % branches, a wide spectrum of spherulite types, ranging from the highly ordered type a to random lamellae (type h) are formed at different temperatures of quenching. Yet, the degree of crystallinity remains continuous with the quenching temperature and does not reflect the changes in morphology. Thus, it may be concluded that the predominant factors in determining the thermodynamic properties of such polymers are the branching concentration and crystallization conditions. Although these factors also determine the nature of the superstructure formed, the latter does not influence the thermodynamic properties in a significant manner. These results are concordant with those reported previously for similarly constituted samples crystallized in a different manner.[92] Furthermore, they are highly relevant to the crystallization of ethylene copolymers that are used in the present study. This is because these copolymers (like the branched polyethylenes from Mandelkern's study[90]) also develop only very low levels of crystallinity over several decades of time,

under isothermal crystallization conditions. Further crystallization occurs on cooling to room temperature (or lower temperatures).

The nature of spherulites developed in a polymer (homo- and/or copolymer) not only affects the thermodynamic properties and morphology of the material, but also bears a strong influence on its mechanical properties. This aspect is not discussed in detail here since it is not the primary goal of the current study. However, it is of utmost importance to understand the relationship between spherulitic superstructures and the ultimate properties of a polymeric material. This topic has been extensively studied by a number of investigators and further details are available in the literature[93,94,95].

2.9.3   Crystallization and Melting Behaviors of Copolymers

From the several discussions so far, it is clear that the crystallization process in ethylene copolymers is considerably different from that of linear polyethylene. In addition, it is well short of the equilibrium predictions of Flory's copolymer crystallization theory. Instead the conditions of crystallization are governed by kinetic factors arising from hindrances to chain transport due to the presence of comonomers. From the arguments and examples presented in Section 2.9.1, it is clear that the comonomers (except methyl branches) are excluded from the crystal. The influence of the co-units on the resulting morphology of the copolymer was detailed in Section 2.9.2. It is also useful to examine the effects of the rejected branches on the level of crystallinity, crystallization temperature as well as on the melting behavior of the crystals. Several examples are available in the literature that illustrate these aspects of the crystallization and melting processes in copolymers, and are briefly revisited in this section.

2.9.3.1   Crystallinity

Alamo *et al.*[68] have compared the crystallinities of copolymers derived from different methods of measurement such as from enthalpy of fusion, from density and

from the Raman internal modes. All three estimates displayed a steady decrease with increasing comonomer content, without however depending on the chemical type of the co-unit. The dependence of crystallinity on comonomer content is associated with the severe restrictions imposed on the length of the crystallizable sequences with the random addition of comonomer units.

Peeters *et al.*[89] have reported that the crystallinities of a series of homogeneous ethylene/1-octene copolymers vary inversely as the number of short chain branches as well as the cooling rate. The effect of cooling rate was most predominant in the lower branched samples, which may crystallize more perfectly if the time available for crystallization is prolonged via a slower cooling rate. No such effect was seen for the highly branched copolymers, since they crystallize with numerous defects and imperfections (due to the presence of branches that disrupt the crystal structure) regardless of the thermal history.

Mathot *et al.*[80] have examined the comonomer effects on the crystallinity of a variety of ethylene copolymers (similar to VLDPE) via thermal analysis studies. The crystallization process in samples with comonomer content < ~5 mole % branches was found to be largely influenced by cooling rate, whereas the higher branch content materials remained mostly invariant. Plots of crystallinity vs. temperature were constructed from the corrected heat capacities. It was noted from these curves that the degree of crystallinity for the more branched samples continued to increase until the glass transition temperature (T_g) was reached. For instance, in an ethylene/1-octene copolymer with 13 mole % branches, the room temperature crystallinity was ~ 14%, whereas at T_g (~ -50°C), it was ~ 25%. This observation verifies the existence of a range of sequence lengths capable of crystallizing at different temperatures, and is also directly responsible for the broad nature of melting and crystallization in these materials. Mirabella *et al.*[82,96] have also observed the broad and multimodal distribution of sequences in the copolymers (similar to LLDPE) by using Temperature Rising Elution Fractionation (TREF). Deblieck and Mathot[81] have also calculated the crystallinities of a series of ethylene/1-octene copolymers. The crystallinities (derived from crystallinity vs. temperature curves) continued to increase until temperatures as low as -60°C. An additional feature of this study is that the samples used were fractionated using a crystallization/dissolution

fractionating procedure into fractions with vastly different melting temperatures, ranging from the poorly crystallizable type up to the ones similar to HDPE. This indicates that the materials used were a blend of a variety of copolymer molecules. It also implies that the heterogeneity in comonomer incorporation was mostly intermolecular in nature rather than being intramolecular.

2.9.3.2   Melting Temperature

In Section 2.6.1 on Flory's crystallization theory for copolymers, an expression for the melting temperature depression of a copolymer with respect to that of a pure homopolymer was derived (Equation (9). According to that expression, the melting point of a copolymer (T_m) does not bear a unique dependence on composition, nor is it significantly influenced by the nature of the co-unit, as long as the comonomer is non-crystallizable and is excluded from the crystal lattice. T_m is influenced mostly by the sequence distribution of the co-unit in the copolymer, represented in the expression as *p*. It has been demonstrated that the melting behaviors of copolymers are independent of the chemical nature of the co-unit (except methyl), provided the sequences are randomly distributed in the copolymer.[38,68,69,72] Significant deviations from the expected behavior have been known to result from the non-random nature of copolymers. A classic example is the comparison of random ethylene/1-octene copolymers with fractions obtained from heterogeneous copolymers via Temperature Rising Elution Fractionation (TREF) by Peeters *et al.*[89] It was noted that the fractions of all comonomer contents had higher melting temperatures (via DSC) than the corresponding copolymers. This result was explained on the basis of the possibility of the copolymers possessing

(a) a more uniform distribution of branches among the different polymer chains than the fractions, and

(b) a random distribution of short chain branches within a single polymer chain.

Hydrogenated polybutadienes (HPBs) are often considered as model random ethylene/1-butene copolymers. They are synthesized via anionic polymerization of

butadiene and possess three types of structural entities- 1, 4-cis units, 1, 4-trans units and 1, 2-vinyl units. The chains containing the vinyl units are converted into the equivalent of an ethylene-1-butene copolymer with a corresponding number of ethyl branches per 1000 backbone carbon atoms. HPBs are characterized by very narrow molecular weight distributions ($M_w/M_n < 1.1$) and compositional homogeneity. Graessley *et al.*[97] have examined the thermal properties of a series of HPBs with 4 to 58 mole % ethyl branches via DSC. The melting temperatures were found to decrease monotonically with increasing branch content. The secondary transition temperature on extrapolation to zero branch content yielded a value equal to -22°C, which is in close agreement with the T_β value of -20°C, reported for linear polyethylene.[98] The glass transition temperature, T_g, also displayed a monotonic decrease with decreasing branch content. This was attributed to the increased difficulty of chain motions with increasing branch concentrations, resulting in higher T_gs. Furthermore, an extrapolation of this T_g to zero branch content yields a value ~ -85°C for the T_g of amorphous polyethylene. Although this value was consistent with a few other[99,100] reported values, it is much lower than the value of T_β observed via mechanical experiments[101,102] for semicrystalline polyethylene. The difference between the two values could be directly related to the immobilization of the amorphous phase by the crystalline regions in the material. The stress-strain properties of the materials were also examined at 23°C, and useful quantities such as tensile (E_s) and other related moduli were estimated. A semilogarithmic variation of E_s with crystallinity was obtained in accordance with the logarithmic mixing laws derived for two-phase semicrystalline systems by Gray and McCrum.[103] However, the value obtained for E_s (at 23°C) on extrapolation to zero crystallinity ($\sim 3\times10^6$ to 4×10^6 Pascal) was about two orders of magnitude lower than the values reported for amorphous polyethylene[104] ($\sim 3\times10^8$ to 4×10^8 Pascal). As before, this was attributed to the excessive restrictions placed on the amorphous phase that is sandwiched between lamellar crystallites.

Alamo and Mandelkern[72] have also reported a decrease in the melting temperatures (T_m) of ethylene/α-olefin copolymers with increasing branch content. However, the T_m's were found to be independent of the chemical nature of the co-unit and significantly lower than those predicted by Flory's theory. The lower values were

attributed to the requirement (in the theory) of total equilibrium throughout the system, which is practically unachievable even under stringent conditions of crystallization.

2.9.3.3   Crystal Parameters - Thickness and Surface Free Energy

It may be recalled from Section 2.7 that the melting temperatures of copolymers are not dictated by undercoolings, unlike those of linear polyethylene. Furthermore, methods such as the Gibbs-Thomson and Hoffman-Weeks extrapolation are no longer applicable for copolymers. In spite of this, a number of investigators have employed these methods to determine the crystal thickness distributions and surface free energies from the melting traces (from thermal analysis) and long periods (from SAXS). A few of these studies are discussed below mainly in view of their conclusions, which are relevant to the present investigation. However, it is noted that the results by no means provide an accurate quantitative representation of the crystal parameters, and therefore must be viewed with caution.

Darras and Seguela[50] have calculated the surface free energies (σ_e) for a series of ethylene/1-butene copolymers using the most probable value of the crystal thickness distribution obtained from SAXS and a T_f^0 value of 140°C. The free energies were found to increase steadily with comonomer concentration indicative of increasing disorder in the amorphous regions. This further implied that the surface free energy of crystals formed from the melt was higher than that of the most stable crystal morphology i.e., regular chain folding. The authors have suggested that increasing comonomer content decreases the possibility of regular chain folding and gives way to random chain folding or even "fringed-micelle macroconformations". Furthermore, the σ_e value calculated for the highest branched copolymer = 0.11J/m^2 was less than the value for fringed-micellar crystals ($\sigma_e = 0.24$J/m^2). This means that even the most branched materials may possess a considerable degree of chain folding (more random than regular). The observations from this study are consistent with previous mechanical investigations by the same group.[105,106] A decrease in drawability and an increase in strain hardening with increasing comonomer content were observed. These effects "were taken as evidence of hindrance to the chain unfolding process"[105] in such copolymers. The authors[50] have

rightly pointed out that the copolymers are far from obeying Flory's model. However, the value of T_f^0 used in the study is larger than that expected for random copolymers of similar composition. This could suggest that the materials employed might not have been completely random. Furthermore, the crystallite thickness distributions calculated from the Gibbs-Thomson equation are not supported by experimental data.

Peeters et al.[89] have reported that the long period (distance from the center of one crystallite to that of another) and the crystal thickness of ethylene/1-octene copolymers were found to decrease with increasing branch content, and exhibit a systematic increase with increasing cooling rate. Alamo et al.[68] have made similar observations on the crystallite thicknesses of copolymers, derived from the peak height of the LAM Raman distribution. These thicknesses for all the copolymers studied, except ethylene/propylene (EP) could be represented by a single curve that decreases with increasing comonomer content. The lower crystal thicknesses at higher branch concentrations are related to the restrictions on sequence lengths in those materials. The higher crystal thicknesses obtained for the EP copolymers are consistent with the inference made earlier that the methyl groups are included in the crystal. The properties of the EP copolymers are more akin to those of homopolymers rather than of random copolymers.[107]

Minick et al.[85] have investigated the effect of comonomers on the crystal thickness and surface order of the copolymer crystals. This was done by estimating an incremental crystal fraction, X, from the DSC melting traces of a series of ethylene copolymers with different branch types. This fraction was plotted as a function of L/σ_e from the Gibbs -Thomson expression. The authors have pointed out that it is more meaningful to consider a ratio of the crystal thickness, L, and the surface free energy, σ_e, rather than the absolute values of either, since both of these quantities are changing with temperature in such copolymers. This ratio also represents the combined effects of the presence of the comonomer on crystal thickness as well as on surface order. The number of peaks obtained in a plot of X vs. L/σ_e was taken as a measure of the types of crystals present in the copolymer. A copolymer with 25 branches per 1000 carbons exhibited two peaks, corresponding to two types of crystal populations; while a copolymer with 38 branches per 1000 carbons had only one peak. These observations were consistent with

the two types of crystals (lamellae and bundled crystals) visible in the micrographs of the former material, and only one (bundles only) for the latter.

2.9.3.4   Effect Of Molar Mass

The influence of molar mass on the crystallization and melting behaviors of random copolymers has been investigated by several workers. Alamo and Mandelkern[72] have reported a decrease in the degrees of crystallinity and melting temperatures of quenched random ethylene-olefin copolymers with increasing molar mass up to 100,000 g/mole, while being independent of comonomer type. Copolymers with different types of branches could be represented by a single curve in the T_m vs. Mw plot, with the curves shifting to lower T_m's for increasing comonomer content. This behavior of random copolymers is in contrast to that observed for quenched linear polyethylene, which shows very little variation of T_m with molar mass. The reduction of T_m with increasing Mw in the case of copolymers may be explained as follows: The increased entanglement density in the melt at higher molar masses considerably slows down the disentanglement of chains and hinders the ability of the chains to participate in the crystal formation process. Thus, the kinetic constraints imposed by the higher molar mass not only reduces the level of crystallinity, but also leads to the formation of thinner and smaller crystals that melt at lower temperatures.

The explanation proposed above is consistent with the results of Peeters *et al.*[89] They observed via SAXS studies that an increase in molar mass of homogeneous ethylene-octene copolymers with a given branch content caused a slight decrease in the crystal thickness, whereas the amorphous thickness exhibited a pronounced increase. Similar results have been recently reported for metallocene-catalyzed linear polyethylenes.[108] This result was explained[89] as being due to the larger number of entanglements present at higher molar masses. These serve to slow down the reptation of polymer chains, thereby causing chain folds to become looser, resulting in a significant increase of the amorphous layer thickness. It has been demonstrated that not only crystallite thicknesses but also the nature of lamellae formed are also influenced to a

significant extent by molar mass and chain length.[72] A deterioration of the long and straight lamellar structure, and a decrease in crystal thickness with increasing chain lengths has been reported for a number of long chain branched copolymers including hydrogenated polybutadienes.[109] The lamellae that were long and straight at a molar mass of 7000 g/mol. have been observed to become short and highly segmented for a mass of 70,000 g/mol. The lateral dimensions of the lamellae are also reported to decrease significantly with molar mass. These results are consistent with the observed decrease of melting temperatures with increasing molar masses for such copolymers.

2.10   Structure

The background and literature detailed in the previous section were focused mainly on calorimetric investigations. However, a sizable part of the present study is related to the structural aspects of the ethylene/α-olefin copolymers determined by means of infrared spectroscopy. As a result, it is useful to review the basic concepts of this technique. Furthermore, in order to aid in the meaningful interpretation of the infrared spectra collected, it is essential to understand the significant features of the polyethylene spectrum, including the influence of different types of branches. These aspects, along with a brief summary of the relevant literature available are discussed in this section.

2.10.1   Theory Of Infrared Spectrsocopy

Infrared spectroscopy (IR) has become one of the most often used spectroscopic techniques because it is a simple, sensitive and relatively inexpensive means of probing the vibrational states of molecules. It is also sensitive to the conformations and packing of these molecules with respect to their environments. This sensitivity is taken advantage of particularly in the study of polymers, where the IR method is widely used to distinguish between bands in the ordered crystalline regions and those in the disordered amorphous regions. Although IR spectroscopy is highly successful in making precise

measurements regarding the relative proportions of different species in a sample, it has not been widely employed in absolute quantitative measurements due to the demanding nature of the process. The absolute values of the degrees of crystallinity and the proportions of different structural forms present in a series of ethylene/α-olefin copolymers are estimated in the present study. It is useful to review the theory of IR spectroscopy before proceeding to the details of the analysis.

The infrared intensity of a band obtained from the experimental spectrum corresponds to the integrated absorbance, A_s, and is given by the following expression.

$$A_s = \left[\frac{1}{cb}\right] \int_{Band} \ln\left(\frac{I_0}{I}\right) dv$$

(18)

$$\Rightarrow A_s = \left[\frac{1}{cb}\right] \int_{Band} A_v dv$$

where $A_v = \ln\left(\frac{I_0}{I}\right)$ = the absorbance at frequency v (in wavenumbers)

c = the concentration (in moles/liter) or density of the sample, and

b = the path length (in cm).

The intensity of IR absorption by a molecule depends on the motions of electronic charges during the vibration of a molecule. Then the infrared absorbance, A_s, can be directly related to the distribution of electronic charges in the molecules, and to the paths adopted for their redistribution during molecular vibrations. Such a relationship is expressed in the form of the equation,

(19)
$$A_s = \left[\frac{8\pi^2 N_A}{3hc_s}\right] v_s \left|\frac{\partial \mu}{\partial Q_s}\right|^2$$

where N_A = Avogadro's number = 6.022×10^{23} mol^{-1}

h = Planck's constant = 6.626×10^{-34} J sec.

c_s = the speed of light = 3×10^{10} cm/sec.

v_s = the frequency of the peak center

μ = the dipole moment of the vibrating species, and

Q_s = the representation of the normal coordinates.

It is seen from this equation that the infrared intensity is significantly influenced even by minor changes in structure and environment of the molecules, e.g., variations in packing density markedly affects the dipole moment of the vibrating species. This relationship forms the basis of the sensitivity of the IR technique to changes at the molecular level.

For applications involving quantitative analysis, the infrared intensity of a vibrational mode is given by Beer's law, represented as:

(20) $A = abc$

where A = the absorbance

a = the absorptivity

b = the path length, and

c = the concentration of the group whose vibrations are considered.

The absorptivity, a, is usually determined prior to the quantitative infrared analysis by calibration with an appropriate standard. Beer's law can also be alternatively expressed in terms of the intrinsic intensity of the band concerned, as:

(21) $I_i^{obsd} \propto x_i I_i^{\mathrm{int}\,r}$

where I_i^{obsd} = the observed intensity of the band associated with the ith component

I_i^{intr} = the intrinsic intensity of the band associated with the ith component, and

x_i = the concentration of the ith component.

In this case, the intrinsic intensities are evaluated from the infrared spectra of suitable standards.

The infrared rays impinging on a sample are subjected to a number of phenomena including reflection, absorption, transmission and scattering. This is mathematically represented by the following expression.

(22) $$I_0 = I_r + I_a + I_t + I_s$$

where I_0, I_r, I_a, I_t and I_s are the intensities of the incident, reflected, absorbed, transmitted and scattered rays respectively. It is possible to use any of the latter four modified radiations to determine the infrared spectrum of a sample, by simply changing the angle of incidence. For instance, transmission spectra are obtained at an angle of incidence equal to 90°, while reflectance spectra correspond to smaller angles. The transmission method is adopted in the present study, since it is characterized by the highest signal-to-noise ratios and easy quantification of the spectra collected.[110] However, the transmission method requires that the samples be completely uniform and thin enough to transmit light and to exhibit absorbance values of less than one. This requirement implies that the sample thicknesses must not exceed the range 10 to 100μm, and that they should be free from holes and other imperfections as well as from gradations in thickness. Such samples were achieved in the current study by a combination of melt pressing followed by slow melting and quenching, as will be described in a following chapter.

2.10.2   Infrared Spectrum Of Polyethylene

Having discussed the basic theory behind infrared spectroscopy, we now proceed to a discussion of the infrared spectrum of polyethylene. This spectrum is rich in information as well as in bands arising from different types of molecular motions involving the methylene group, such as rocking, wagging, scissoring, etc. The intensities of the bands due to the above motions are well characterized for this material, and may be used in the determination of the amount of crystal and amorphous fractions present in the

sample. Since the goal of the present study is to determine the absolute values of the degrees of crystallinity of the copolymers as a function of branch concentration and of temperature, only those bands that are directly related to the these aspects are included in the discussion.

Specific bands that enable the characterization of both the crystalline as well as the amorphous fractions of polyethylene are present in the 735 to 715 cm^{-1} region of the spectrum. Two peaks appearing at 730 and 722 cm^{-1} are associated with the crystalline fraction. The assignment is based on the appearance of the two peaks in the IR spectra of *n*-paraffins with the orthorhombic structure, as well as in the spectra of highly crystalline polyethylene.[111,112] These peaks are fairly narrow with characteristic half-widths of ~ 2 cm^{-1} at room temperature. A much broader peak of half-width ~ 20 cm^{-1} appears at 723 cm^{-1} and is associated with the disordered amorphous phase.[113] All three peaks are assigned to the rocking mode of the methylene sequences. It is evident that the amorphous band at 723 cm^{-1} presents a considerable degree of overlap with the crystalline peak at 722 cm^{-1}. Therefore, any attempt to evaluate the crystallinity values from the intensities of these peaks must involve a deconvolution process to separate the contributions of the crystalline and amorphous fractions. In the present study, such a deconvolution is achieved by means of curve-fitting procedures. It must also be mentioned that the widely different widths of the peaks involved enables an efficient separation via curve fitting. The degree of crystallinity, χ_c, of a sample estimated from the intensities of the bands in this region is given by the relationship,[114]

$$(23) \qquad \chi_c = \frac{I_{722} + I_{730}}{I_{722} + I_{730} + \alpha I_{723}}$$

where I refers to the intensity of the corresponding bands. The coefficient α is included to account for the fact that the intrinsic intensities of the crystalline and amorphous bands are not exactly identical to each other. A mathematical expression for α is given below.[114] The value of this coefficient has been determined to be equal to 1.2, from intensity measurements.

$$\alpha = \frac{I_{722}^{\text{int}\,r} + I_{730}^{\text{int}\,r}}{I_{723}^{\text{int}\,r}}$$

A similar set of three bands is present in the 1475 to 1420 cm^{-1} region of the spectrum, which is assigned to the methylene scissoring mode. Two narrow bands of half-widths ~ 2 cm^{-1} appear at 1473 and 1463 cm^{-1}, and are assigned to the crystalline fraction. A much broader band of half-width ~ 15 cm^{-1} is found to appear at 1476 cm^{-1}, overlapping the crystalline peaks. This broad band is associated with the amorphous portion of the material. The shapes and overlapping nature of the above peaks are similar to those of the bands in the 735 to 715 cm^{-1} region discussed above. However, a major difference lies in the fact that the amorphous band in the higher wavenumber region is highly asymmetric. This introduces further difficulties in the curve fitting procedure in this region. As a result, the crystallinity values derived from this region are less accurate and less reliable than those obtained from the 735 to 715 cm^{-1} bands.

Another set of bands appearing in the 1400 to 1250 cm^{-1} region is used in the determination of the amorphous content of the samples. These have been associated with short conformational sequences involving gauche bonds in the disordered amorphous regions[113].

Snyder[113] has performed a detailed conformational analysis of liquid *n*-paraffins ranging from C$_4$ to C$_{17}$ and molten polyethylene by means of a valence force field that was applicable to both planar and non-planar chains. This field was developed based on the idea that a vibrational mode that is localized in one part of an *n*-paraffin molecule will also be localized in an infinite chain, part of whose conformation resembles that of the above-mentioned portion of the *n*-paraffin. Furthermore, this method is an improvement over the previously reported field for extended *n*-paraffins by the same author.[115] The different trans and gauche states of the bonds, and the infrared frequencies associated with the rotational isomeric states are extensively investigated. In comparing the spectra of the *n*-paraffins to polyethylene, it was found that the bands present could be classified into three types, based on their frequencies and intensities:

1. Bands whose frequencies were found to be chain length dependent - The number of such bands increased with increasing chain length, leading to a great degree of overlap with each other

2. Bands whose intensities decreased with increasing chain length, while their frequencies remained constant - These bands were related to the end group vibrations, and

3. Bands whose frequencies as well as intensities remained practically invariant with chain length.

Further details of the analysis are not discussed here. However, a comprehensive knowledge of the infrared behavior of the different conformations of polyethylene may be gained by referring to Snyder's review.[113]

2.10.3   Influence Of Branches On The Infrared Spectra

Different types of branches attached to the polyethylene backbone can give rise to specific bands in the infrared spectrum. These bands may be used to identify the nature of the comonomer present in the material. This aspect is highly relevant to the present study involving ethylene/α-olefin copolymers of different branch lengths, and is discussed at some length below. McRae and Maddams[116] have published a detailed report on the infrared characteristics of a few specific short branches. According to their results, the methyl branch may be clearly identified by a band at 935 cm^{-1}, assigned to the methyl rocking mode. The intensity of this band was found to increase linearly with increasing concentration of the methyl branches. The use of this band provides a means of quantitative identification of the methyl group concentration down to the level of two methyl branches per 1000 carbon atoms. Such a characterization of the methyl branch is also possible from the intensity of the 1150 cm^{-1} band, assigned to the methyl wagging mode.[117]

In contrast, the ethyl groups resulted in a very weak band at 910 cm^{-1}, also assigned to the rocking mode. In addition to being weak, this band coincides with the strong absorption peaks due to the residual vinyl groups in certain commercial

polyethylenes. As a result, it was concluded that the identification of ethyl groups is not possible by means of the 910 cm^{-1} band. However, the ethyl branches may be characterized by a band at 780 cm^{-1} due to the rocking mode vibration of the methylene groups present in the ethyl branches.

Longer branches including propyl, butyl, pentyl and hexyl exhibit a band at 890 cm^{-1} arising from the methyl rocking mode. Although this band can be used as an indication of the presence of one or more of the above branches, it cannot be used to characterize the specific nature of the branch present. Samples with these longer branches yielded a few weak bands in the spectral region around 1150 cm^{-1} (characterized by the methyl wagging mode). However, the authors warn against the use of such bands for characterization purposes, due to the high degree of interference from oxygenated species and polyethylene oxidation products that strongly absorb in that region.

The above discussion was specific to the short branches that are of immediate relevance to the present study. A detailed survey of the frequency and intensity data of a variety of group vibrations has been made available by Wexler.[118]

2.10.4   Structure Of Polyethylene

A proper understanding of the physical properties of bulk polymers demands a detailed knowledge of their fine structure, which involves the relative positions of the carbon atoms in the molecular chains. Such information had become sought after as early as 1945, as represented by the early X-ray diffraction studies on polyethylene films by Bunn.[119,120] It was estimated from powder diffraction patterns that four methylene groups were present per unit cell of polyethylene. Further analysis revealed that the only structure that satisfied the above finding as well as the bond distance and valence angle requirements for aliphatic compounds was the orthorhombic space group. This structure was also consistent with the generally accepted structure of crystalline *n*-paraffinic hydrocarbons,[121] and has since then been assigned as the primary crystal structure for linear polyethylene. This structure is schematically depicted in Figure 9.

The orthorhombic unit cell of polyethylene, as shown in Figure 10 consists of five molecules - one at the center and the other four at the corners of the unit cell. The four corner molecules are each equally shared with four other unit cells, thereby reducing the contribution of each molecule to a given cell. In effect, a unit cell may be considered to be made up of contributions by two molecules obtained as 1+ (4×1/4). The contribution to the net dipole moment of the unit cell by the two molecules also follows the same splitting. The symmetry of the factor group for polyethylene permits the two molecules to vibrate with only two different phase relationships - one where the overall dipole moment is parallel to the b axis, and the other where it is parallel to the a axis[122]. These two possibilities are depicted in Figure 10 and are responsible for the strong doublet observed at 720/730 cm^{-1} in the infrared spectrum of polyethylene, which is assigned to the CH_2 rocking mode. Measurements using plane polarized radiation on biaxially oriented polyethylene samples showed that the dipole moment change parallel to the b axis results in the peak at 720cm^{-1} and the peak at 730cm^{-1} originates from the dipole moment change parallel to the a axis.
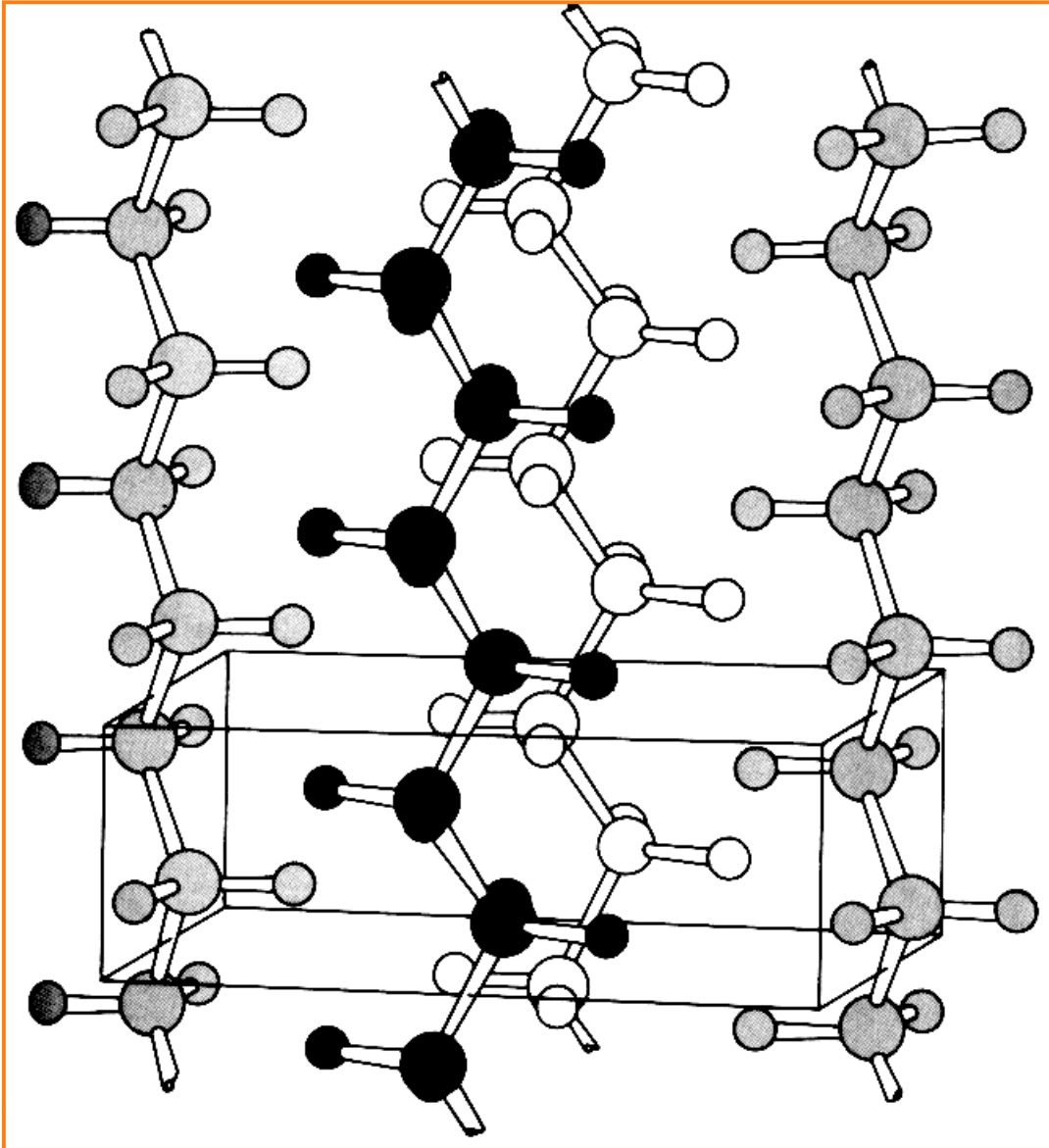
Figure 9 Orthorhombic crystal structure for polyethylene (Adopted from Ref.2)
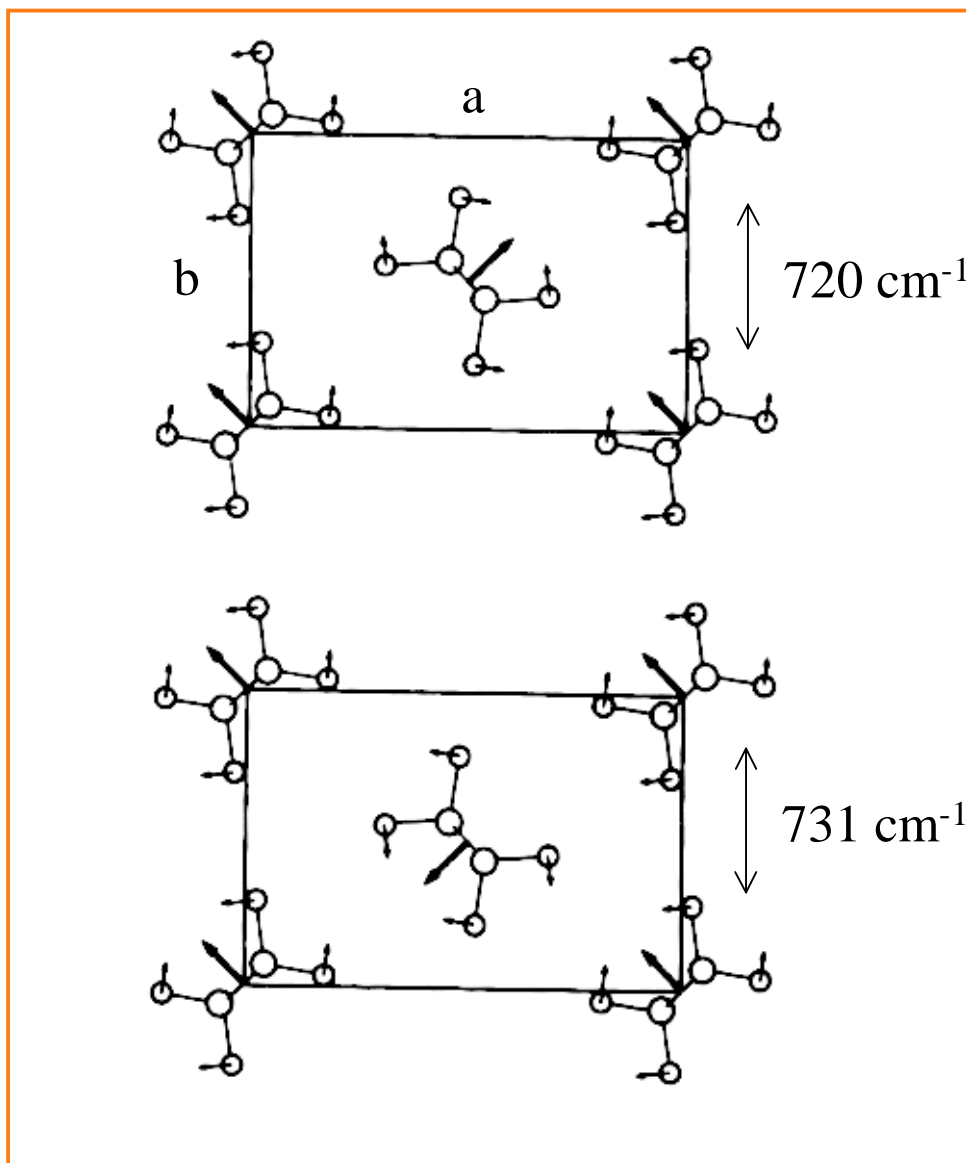
Figure 10 The two allowed phase relationships of chain vibrations in the unit cell of polyethylene. The short arrows represent the direction of motion of the corresponding atoms. The long and broad arrows represent the direction of the instantaneous dipole moment (Adopted from Ref. 122)

Although the orthorhombic structure is the predominantly assigned primary structure for polyethylene, indications of other crystal structures have been reported since the early 1960's, via Wide Angle X-Ray Diffraction studies on polyethylene.[123,124,125] Fatou *et al*.[126] have carried out a detailed investigation on the effects of crystallization conditions on this second structure (discerned as an extra reflection in the WAXD spectrum) of polyethylenes spanning a broad range of molecular weights. It was observed that increasing the molecular weight causes the reflection to transform from a very sharp feature to a very diffuse and broad halo. The influence of cooling rate was also significant, with no extra reflections being observed for quenched and rapidly cooled samples. However, annealing the quenched samples resulted in the reappearance of the feature, which progressively weakened at higher annealing temperatures, until it became almost undetectable at a certain temperature. These results were further substantiated by dilatometric studies that revealed a definite discontinuity at the temperature of disappearance of the reflection (from WAXD). However, no clear transitions were observed at these temperatures from the fusion curves of the samples. Based on these observations, the authors unequivocally assert the existence of a second crystal structure in polyethylene, without presenting a conclusive relationship between the nature of this form and other physical and mechanical properties of the sample. Further evidence for the presence of a second crystal structure in polyethylene is derived from the studies of Teare and Holmes,[125] wherein the extra reflections in WAXD spectra are assigned to a triclinic structure. This assignment is related to the fact that the second crystal structure found in polyethylene was similar to the triclinic form of *n*-paraffins.[127,128] However, this crystal structure has also been associated with a monoclinic unit cell structure.[129,130] Since then, a number of investigations have revealed the presence of the monoclinic phase in polyethylene crystallized under different conditions. The results from a few of those studies are discussed below.

Kikuchi and Krimm[131] have studied the transformation from the orthorhombic to the monoclinic crystal structure in single crystals of polyethylene. The single crystals were shaken in a vibratory grinder for ~ 90 seconds at room temperature, after which their infrared spectra were collected. A new absorption band appeared as a shoulder near 715 cm^{-1} in the methylene rocking region, in addition to the 730/720 cm^{-1} doublet

associated with the orthorhombic phase. The authors assigned this band that was induced by shear to the monoclinic cell structure based on previous reports of the infrared spectra of *n*-paraffins in the monoclinic form.[132,133] These paraffins were found to exhibit a single band at 715-718 cm^{-1} in the rocking region. The band at 715cm^{-1} in the above study was found to disappear upon annealing of the crystals at temperatures as low as 70°C. This observation may be related to the higher degree of disorder associated with the monoclinic crystals. Since annealing allows the chains to rearrange into more ordered structures, it follows that the transformation from monoclinic to the more ordered orthorhombic phase can easily occur under these conditions. This observation is also in agreement with the results from WAXD on single crystals[123] of polyethylene. It was reported in these studies that the X-ray spectrum of a shaken sample displayed a new line at ~ 4.6Å, in addition to the usually expected features of the orthorhombic structure. This line, which was attributed to the presence of a second (monoclinic) phase in the sample, was seen to disappear when the crystals were annealed at different temperatures.

In a more recent study, Hagemann *et al.*[114] have measured the temperature dependence of crystallinity of polyethylenes crystallized under different conditions. They used an expression to determine the above quantity, starting from Beer's law as represented in Equation (21). Differentiation of this equation with respect to temperature yields,

$$\frac{\partial \ln I_i^{obsd}}{\partial T} = \frac{\partial \ln x_i}{\partial T} + \frac{\partial \ln I_i^{int\,r}}{\partial T}$$

where *i* could represent either the crystalline or the amorphous component of the samples. Then, the temperature coefficient of crystallinity is obtained from the above relationship and is shown below. (A similar expression for the amorphous fraction is given by using the subscript, *a* for amorphous fraction, in place of the subscript *c* in the following expression).

$$(24) \qquad \frac{\partial \ln x_c}{\partial T} = \frac{\partial \ln I_c^{obsd}}{\partial T} - \frac{\partial \ln I_c^{int\,r}}{\partial T}$$

The first term on the right hand side of the above equation is directly measured from the intensity of the corresponding band in the infrared spectrum. The second term, related to the intrinsic intensity, is measured from the intensity of the same band in the spectrum of an appropriate standard material. For instance, the standard used in Hagemann's study is a liquid n-alkane, n-$C_{16}H_{34}$. The choice of the standard was made based on the conclusions of calculations made using the rotational isomeric state model.[134] It was concluded that the trans/gauche bond ratios and their temperature coefficients for liquid n-$C_{16}H_{34}$ are not significantly different from the values for lengthy polymer chains with the same repeating sequences.

Furthermore, an expression for the temperature dependence of the amorphous content was obtained from Equation (24), also based on the condition, $x_c + x_a = 1$ for a semicrystalline polymer. This is given below.

(25) $$x_c \frac{\partial \ln x_c}{\partial T} + x_a \frac{\partial \ln x_a}{\partial T} = 0$$

The temperature coefficients of crystallinity calculated using the above equations were found to increase significantly with decreasing the crystallinities. This variation is a direct implication of the increasing breadth of the fusion process in high molecular weight linear polymers and copolymers. In such materials, a range of sequence lengths exists, giving rise to crystals that melt over a range of temperatures. These crystals are less stable than those found in linear polyethylene, which show very little melting until high temperatures are reached.

The temperature coefficients of crystallinity were also found to increase with increasing temperature, for all the samples examined. This variation was directly related to the partial melting of the samples below their melting temperatures. However, as the melting temperatures of the samples were approached, the coefficients tended toward a common value. Based on the magnitude and slope of the temperature variation of this coefficient, the authors proposed that it played a significant role in determining the temperature dependence of the specific volume of the samples. This idea is supported by previous reports on samples similar to the one used in the above study.[135,136] These

reports indicate that the temperature variation of the specific volume of the sample and that of the crystalline fraction therein have identical slopes in the temperature range -150 to 0°C. At higher temperatures, the semicrystalline sample begins to show higher slopes than the crystalline fraction. Based on the idea proposed by the above authors, this observation is explained on the basis of increasing extent of partial melting (also called premelting) with increasing temperatures. At temperatures higher than 0°C, there is a significantly greater increase in the amorphous fraction (due to premelting) compared to the crystalline fraction.

Another interesting observation was made in Hagemann's[114] study. The integrated intensities of the amorphous bands were found to first decrease, and then increase with increasing temperatures. Such a variation with a minimum at a certain temperature is in contrast to the expected increase in amorphous band intensity with increasing temperatures. Similar results, have however been reported by Dahme and Dechant[137] for semicrystalline polyethylene. Hagemann *et al.*[114] have proposed an explanation for this anomalous behavior based on the amorphous counterpart of Equation (24), which is given below for comparison.

$$\frac{\partial \ln I_a^{obsd}}{\partial T} = \frac{\partial \ln x_a}{\partial T} + \frac{\partial \ln I_a^{\text{int}\,r}}{\partial T}$$

This equation predicts the temperature dependence of the amorphous intensity as the sum of two terms. The intrinsic intensity (second term on the right hand side) decreases with temperature and is predominant at lower temperatures. However, the amorphous content (first term on the right hand side) increases with temperature and dominates the behavior at higher temperatures. Thus, it is evident that the observed amorphous intensity must equal zero (go through a minimum) at a certain temperature. This minimum has been experimentally found to shift to lower temperatures with decreasing crystallinities. An easy explanation is provided based on the onset of partial melting at lower temperatures in samples of lower degrees of crystallinity.

2.10.5   Structure Of Copolymers Via WAXD

Mathot *et al.*[80] have reported that the WAXD patterns of a series of ethylene/1-octene copolymers show steadily decreasing crystal reflections with increasing comonomer content, until no reflections are observed for the highest branched copolymer. This result was explained on the basis of the decreasing dimensions of the crystalline structures in conjunction with imperfections. These factors were found to be responsible for the absence of constructive interference and thereby crystal reflections. They further suggested that the density of such imperfect and small crystals could be lower than that of the perfect orthorhombic crystal structure associated with polyethylene. The authors derive additional support from Monte Carlo simulations on crystal structures obtained with different comonomer contents in such copolymers.[138] The morphology was indicative of a fairly open structure, comprised of loosely organized clusters of ethylene sequences. The boundaries and regions were not clearly distinguishable and the validity of the applicability of the term "crystallites" was ambiguous. Furthermore, the simulations for the highest comonomer containing materials were suggestive of sheaf-like growth. Then the possibility of a lower density referred to above is not totally baseless.

This result is also directly related to the present study on similar copolymers. The possibility of a transformation in unit cell structure from orthorhombic to monoclinic (or hexagonal) on increasing the branch concentration is explored. The higher degree of disorder associated with the latter crystals could also result in lower density for this structure, compared to the more ordered orthorhombic crystals.

Peeters *et al.*[89] have determined the unit cell parameters of ethylene-octene copolymers such as those used in the previous study.[80] These parameters have been estimated from the predominant reflections observed in the WAXD patterns of the copolymers. An increase in branch content causes the length of the *a*-axis to increase significantly, while that of the *b* axis is not too sensitive. This is further reflected in the observed decrease in mass density of the crystalline phase with increasing branch content. However, the lengths of both the *a* and *b* axes increase with increasing molar mass and cooling rate. At this point, it must be mentioned that some authors[139,140,141,142] have interpreted the *a*-axis expansion and the accompanying decrease in crystallite

thickness as an indication that the branches are incorporated into the crystal lattice.   Such a conclusion is not a definite and necessary consequence of the above observations. The decrease in crystal thickness could be a direct result of the disordering in sequence distribution caused by branching. The expansion of the *a*-axis could be a result of the increased strain resulting from the aggregation of the co-units at the interface of the thin crystals.[143]

Thus, the significant aspects related to the crystallization behavior, microstructure and structural features of the random copolymers of the type used in the present study have been reviewed. The theories modeling the crystallization of homo as well as copolymers have been presented in comparison to one another. The contents of this section are meant to aid in understanding the implications of the results obtained from the experiments that follow. This is certainly not a complete discussion of the highly complex phenomena involved in the crystal forming processes. Further details are available in the appropriate references.[1,2,3,7,11,61,62,77,110,111,122]

[1] P. J. Flory, "*Principles of Polymer Chemistry*", Cornell University Press, Ithaca, N.Y., 1953

[2] L. Mandelkern, "*An Introduction to Macromolecules*", Springer-Verlag, N.Y., 1983

[3] L. Mandelkern, "*Crystallization of Polymers*", McGraw-Hill Book Company, N.Y., 1964

[4] L. Mandelkern, "*The Crystalline State*" in *Physical Properties of Polymers*, Ed., J. E. Mark, ACS Washington D.C. (1984)

[5] A. Keller, *Phil. Mag.*, **2**, 1171 (1957)

[6] A. Keller, *Rep. Prog. Phys.*, **31**, 623 (1968)

[7] F. Khoury and E. Passaglia, "*Treatise on Solid State Chemistry*", Ed., N. B. Hannay, Plenum Press, New York, Vol. 3, Pg. 335-496 (1976)

[8] R. Patil and D. H. Reneker, *Polymer*, **35**, 1909 (1994)

[9] J. C. Wittmann and B. Lotz, *J. Polym. Sci. Polym. Phys. Ed.*, **23**, 205 (1985)

[10] P. J. Flory, *J. Am. Chem. Soc.*, **84**, 2858 (1962)

[11] A. E. Woodward, "*Atlas of Polymer Morphology*", Hanser, Munich (1988)

[12] J. M. Schultz and R. D. Scott, *J.Polym. Sci. A-2*, **7**, 659 (1969)

[13] J. D. Hoffman and J. J. Weeks, *J. Chem. Phys.*, **42**, 4301 (1965)

[14] B. Wunderlich and J. Mellilo, *Macromol. Chem.*, **118**, 250 (1968)

[15] W. Banks, M. Gordon, R. J. Roe and A. Sharples, *Polymer*, **4**, 61 (1963)

[16] F. Rybnikar, *J. Polym. Sci.*, **44**, 517 (1960)

[17] E. W. Fischer and G. F. Schmidt, *Angew. Chem. (Intern. Ed. Engl.)*, **1**, 488 (1962)

[18] E. W. Fischer, *Pure Appl. Chem.*, **31(1)**, 113 (1972)

[19] D. T. Grubb, J. H. Liu, M. Caffrey and D. H. Bilderback, *J. Polym. Sci. Polym. Phys. Ed.*, **22**, 367 (1984)

[20] R. L. Collins, *J. Polym. Sci.*, **27**, 75 (1958)

[21] J. P. Bell and T. Murayama, *J. Polym. Sci. Part A-2*, **7**, 1059 (1969)

[22] S. Fakirov, E. W. Fischer, R. Hoffmann and G. F. Schmidt, *Polymer*, **18**, 1121 (1977)

[23] E. W. Fischer and S. Fakirov, *J. Mat. Sci.*, **11**, 1041 (1976)

[24] G. Groeninckx, H. Reynaers, H. Berghmans and G. Smets, *J. Polym. Sci. Polym. Phys. Ed.*, **18**, 1311 (1980)

[25] P. J. Flory, *J. Chem. Phys.*, **17**, 3, 223 (1949)

[26] R. Chiang and P. J. Flory, *J. Am. Chem. Soc.*, **83**, 2857 (1961)

[27] J. I. Lauritzen Jr. and J. D. Hoffman, *J. Res. Natl. Bur. Std. (U.S.)*, **64A**, 73 (1960)

[28] J. I. Lauritzen Jr. and J. D. Hoffman, *J. Appl. Phys.*, **44**, 4340 (1973)

[29] J. I. Lauritzen Jr., *J. Appl. Phys.*, **44**, 4353 (1973)

[30] J. D. Hoffman, *Polymer*, **24**, 3 (1983)

[31] J. D. Hoffman, R. L. Miller, H. Marand and D. B. Roitman, *Macromolecules*, **25**, 2221 (1992)

[32] J. H. Gibbs, *"Collected Works"*, Longman Green & Company, Essex, U. K., 1928

[33] J. D. Hoffman, *Soc. Plast. Eng. Trans.*, **4**, 315 (1964)

[34] K. Mezghani, R. A. Campbell and P. J. Phillips, *Macromolecules*, **27**, 997 (1994)

[35] P. J. Flory, *Trans. Faraday Soc.*, **51**, 848 (1955)

[36] B. Crist and P. R. Howard, *Macromolecules*, **32**, 3057 (1999)

[37] C. H. Baker and L. Mandelkern, *Polymer*, **7**, 7 (1966)

[38] M. J. Richardson, P. J. Flory and J. B. Jackson, *Polymer*, **4**, 221 (1963)

[39] I. C. Sanchez and R. K. Eby, *Marcomolecules*, **8**, 638 (1975)

[40] I. C. Sanchez and R. K. Eby, *J. Res. Natl. Bur. Std.-A. Phys. & Chem.*, **77A**, 353 (1973)

[41] T. Pakula, *Polymer*, **23**, 1300 (1982)

[42] T. Pakula and M. Kryszewski, *Euro. Polym. J.*, **12**, 47 (1976)

[43] P. Wang and A. Woodward, *Macromolecules*, **20**, 1818 (1987)

[44] P. Wang and A. Woodward, *Macromolecules*, **20**, 1823 (1987)

[45] E. Helfand and J. I. Lauritzen, Jr., *Macromolecules*, **6**, 631 (1973)

[46] J. I. Lauritzen, Jr., E. A. DiMarzio and E. Passaglia, *J. Chem. Phys.*, **45**, 4444 (1966)

[47] A. Wlochowicz and M. Eder, *Polymer*, **25**, 1268 (1984)

[48] N. Alberola, J. Y. Cavaille and J. Perez, *J. Polym. Sci. Polym. Phys. Ed.*, **28**, 569 (1990)

[49] P. J. Mills and J. N. Hay, *Polymer*, **25**, 1277 (1984)

[50] O. Darras and R. Seguela, *Polymer*, **34**, 2946 (1993)

[51] H. Zhou and G. L. Wilkes, *Polymer*, **38**, 5735 (1997)

[52] L. Lu, R. G. Alamo and L. Mandelkern, *Macromoelcules*, **27**, 6571 (1994)

[53] L. Mandelkern, M. Hellmann, D. W. Brown, D. E. Roberts and F. A. Quinn, Jr., *J. Am. Chem. Soc.*, **75**, 4093 (1953)

[54] R. G. Alamo, E. K. M. Chan, L. Mandelkern and I. G. Voigt-Martin, *Macromolecules*, **25**, 6381 (1992)

[55] B. Crist and G. D. Wignall, *J. Appl. Cryst.* , **21**, 701 (1988)

[56] K. Ziegler, E. Holzkamp, H. Breil and H. Martin, *Angew. Chem.*, **67**, 541 (1955)

[57] G. Natta, P. Pino, P. Corradini, F. Danusso, E. Mantica, G. Mazzanti and G. Moraglio, *J. Am. Chem. Soc.*, **77**, 1708 (1955)

[58] G. Natta, *J. Polym. Sci.*, **16**, 143 (1955)

[59] J. P. Hogan and R. L. Banks, *US Pat.*, 2825721 (1954)

[60] A. Clark, J. P. Hogan, R. L. Banks and W. C. Lanning, *Ind. Eng. Chem.*, **48**, 1152 (1956)

[61] P. J. T. Tait and I. G. Berry in *Comprehensive Polymer Science: The Synthesis, Characterization, Reactions & Applications of Polymers,* Ed., G. C. Eastmond, A. Ledwith, S. Russo and P. Sigwalt, Pergamon Press, **4**, 580 (1989)

[62] F. Ciardelli and C. Carlini in *Comprehensive Polymer Science: The Synthesis, Characterization, Reactions & Applications of Polymers,* Ed., G. C. Eastmond, A. Ledwith, S. Russo and P. Sigwalt, Pergamon Press, **4**, 68 (1989)

[63] P. Pino, U. Giannini and L. Porri in *Encyclopedia of Polymer Science & Engineering*, Ed., H. F. Mark, N. M. Bikales, C. G. Overberger, G. Menges and S. I. Kroschwitz, Wiley, New York, **8**, 147 (1985)

[64] P. Pino, A. Oschwald, F. Ciardelli, C. Carlini and E. Chiellini in *Coordination Polymerization of α-Olefins*, Ed., J. C. W. Chien, Elsevier, New York, p. 25, (1975)

[65] H. Sinn, W. Kaminsky, H. J. Vollmer and R. Woldt, *Angew. Chem., Int. Ed. Engl.*, **19**, 390 (1980)

[66] *Polymeric Materials Encyclopedia*, Ed-in-Chief: Joseph. C. Salamone, Vol. **6**, Pg. 4175, CRC Press (1996)

[67] E. T. Hseih, C. C. Tso, J. D. Byers, T. W. Johnson, Q. Fu and S. Z. D. Cheng, *J. Macromol. Sci. - Phys.,* **B36**, 615 (1997)

[68] R. Alamo, R. Domszy and L. Mandelkern, *J. Phys. Chem.*, **88**, 6587 (1984)

[69] R. G. Alamo and L. Mandelkern, *Macromolecules*, **22**, 1273 (1989)

[70] W. Kaminsky, H. Hahnsen, K. Kulper, R. Woldt, *US Patent 4,542,199* (1985)

[71] S. D. Clas, D. C. McFaddin, K. E. Russell, M. V. Scannell-Bullock and I. R. Peat, *J. Polym. Sci.: Polym. Chem. Ed.*, **25**, 3105 (1987)

[72] R. G. Alamo and L. Mandelkern, *Thermochim. Acta*, **238**, 155 (1994)

[73] D. J. Cutler, P. J. Hendra, M. E. A. Cudby and H. A. Willis, *Polymer*, **18**, 1005 (1977)

[74] J. Vile, P. J. Hendra, H. A. Willis, M. E. A. Cudby and G. Gee, *Polymer*, **25**, 1173 (1984)

[75] C. France, P. J. Hendra, W. F. Maddams and H. A. Willis, *Polymer*, **28**, 710 (1987)

[76] M. Glotin and L. Mandelkern, *Colloid & Polym. Sci.*, **260**, 182 (1982)

[77] L. Mandelkern and A. J. Peacock, "*Studies in Physical and Theoretical Chemistry*", Ed., R. C. Lacher, Elsevier Science Publisher, New York, Vol. 54, p. 201 (1988)

[78] P. J. Flory and A. D. McIntyre, *J. Polym. Sci.*, **18**, 592 (1955)

[79] M. Takayanagi and T. Yamashita, *J. Polym. Sci.*, **22**, 552 (1956)

[80] V. B. F. Mathot, R. L. Scherrenberg and T. F. J. Pijpers, *Polymer*, **39**, 4541 (1998)

[81] R. A. C. Deblieck and V. B. F. Mathot, *J. Mat. Sci. Let.*, **7**, 1276 (1988)

[82] F. M. Mirabella Jr., S. P. Westphal, P. L. Fernando, E. A. Ford and J. G. Williams, *J. Polym. Sci.: Polym. Phys.*, **26**, 1995 (1988)

[83] C. B. Bucknall, "*Toughened Plastics*", Applied Science Publishers, London, p. 185, 1977

[84] K. Sehanobish, R. M. Patel, B. A. Croft, S. P. Chum and C. I. Kao, *J. Appl. Polym. Sci.*, **51**, 887 (1994)

[85] J. Minick, A. Moet, A. Hiltner, E. Baer and S. P. Chum, *J. Appl. Polym. Sci.*, **58**, 1371 (1995)

[86] F. C. Frank and M. Tossi, *Proc. R. Soc. Lond. A*, **263**, 323 (1961)

[87] F. Defoor, G. Groeninckx, P. Schouterden and B. van der Heijden, *Polymer*, **33**, 3879 (1992)

[88] H. G. Zachmann, *Pure Appl. Chem.*, **38**, 79 (1974)

[89] M. Peeters, B. Goderis, C. Vonk, H. Reynaers and V. Mathot, *J. Polym. Sci., Part B: Polym. Phys.*, **35**, 2689 (1997)

[90] L. Mandelkern and J. Maxfield, *J. Polym. Sci. Polym. Phys. Ed.*, **17**, 1913 (1979)

[91] L. Mandelkern, M. Glotin and R. A. Benson, *Macromolecules*, **14**, 22 (1981)c

[92] L. Mandelkern, *Faraday Discuss. Chem. Soc.*, **68**, 310 (1980)

[93] S. Bensason, S. Nazarenko, S. Chum and E. Baer, *Polymer*, **38**, 3513 (1997)

[94] S. Bensason, E. V. Stepanov, S. Chum and E. Baer, *Macromoleucles*, **30**, 2436 (1997)

[95] A. Shah, E. V. Stepanov, E. Baerand M. Klein, *Internat. J. Fract.*, **84**, 159 (1997)

[96] F. M. Mirabella and E. A. Ford, *J. Polym. Sci.: Polym. Phys.*, **25**, 777 (1987)

[97] T. M. Krigas, J. M. Carella, M. J. Struglinski, B. Crist, W. W. Graessley and F. C. Schilling, *J. Polym. Sci. Polym. Phys. Ed.*, **23**, 509 (1985)

[98] R. Popli and L. Mandelkern, *Polym. Bull.*, **9**, 260(1983)

[99] R. Lam and P. H. Geil, *Macromol. Sci. - Phys.*, **B20**, 37 (1981)

[100] J. J. Maurer, *Rubber Chem. Tech.*, **38**, 979 (1965)

[101] H. G. McCrum, B. E. Read and G. Williams, *Anelastic and Dielectric Effects in Polymeric Solids*, Wiley, New York, p. 353-376, 1967

[102] G. T. Davis and R. K. Eby, *J. Appl. Phys.*, **44**, 4274 (1973)

[103] R. W. Gray and N. G. McCrum, *J. Phys. Sci., A-2*, **7**, 1329 (1969)

[104] R. H. Boyd, *J. Polym. Sci., Polym. Phys. Ed.*, **21**, 493 (1983)

[105] R. Seguela and F. Rietsch, *Polymer*, **27**, 703 (1986)

[106] R. Seguela and F. Rietsch, *J. Mat. Sci.*, **23**, 415 (1988)

[107] G. Capaccio and I. M. Ward, *J. Polym. Sci. Polym. Phys. Ed.*, **22**, 475 (1984)

[108] K. Jordens, G. L. Wilkes, J. Janzen, D. C. Rohlfing and M. B. Welch, *Submitted to Polymer*

[109] R. G. Alamo, E. K. M. Chan, L. Mandelkern and I. G. Voigt-Martin, *Macromolecules*, **25**, 6381 (1992)

[110] J. L. Koenig, "*Spectroscopy of Polymers*", American Chemical Society, Washington, DC. (1992)

[111] R. G. Snyder, "*Methods of Experimental Physics*", Eds., L. Marton and C. Marton, Academic Press, New York, Vol. 16; Part A, Chapter 3 (1980)

[112] R. G. Snyder, *J. Mol. Spectrosc.*, **7**, 116 (1961)

[113] R. G. Snyder, *J. Chem. Phys.*, **47**, 1316 (1967)

[114] H. Hagemann, R. G. Snyder, A. J. Peacock and L. Mandelkern, *Macromolecules*, **22**, 3600 (1989)

[115] J. H. Schachtschneider and R. G. Snyder, *Spectrochim. Acta*, **19**, 117 (1963)

[116] M. A. McRae and W. F. Maddams, *Die Makromol. Chem.*, **177**, 449 (1976)

[117] C. Baker and W. F. Maddams, *Die Makromol. Chem.*, **177**, 437 (1976)

[118] A. S. Wexler, *Appl. Spectrosc. Rev.*, **1(1)**, 29 (1967)

[119] C. W. Bunn and T. C. Alcock, *Trans. Faraday Soc.*, **41**, 317 (1945)

[120] C. W. Bunn, *Trans. Faraday Soc.*, **35**, 482 (1939)

[121] A. Muller, *Proc. R. Soc. London*, **A120**, 137 (1928)

[122] D. I. Bower and W. F. Maddams, "*The Vibrational Spectroscopy of Polymers*", Ed., R. W. Cahn, E. A. Davis and I. M. Ward, Cambridge University Press, Cambridge, 1989

[123] A. T. Jones, *J. Polym. Sci.*, **62**, 553 (1962)

[124] S. S. Pollack, W. H. Robinson, R. Chiang and P. J. Flory, *J. Appl. Phys.*, **33**, 237 (1962)

[125] P. W. Teare and D. R. Holmes, *J. Polym. Sci.*, **24**, 496 (1957)

[126] J. G. Fatou, C. H. Baker and L. Mandelkern, *Polymer*, **6**, 243 (1965)

[127] A. Muller and K. Lonsdale, *Acta Cryst.*, **1**, 129 (1948)

[128] T. Hayashida, *J. Phys. Soc. Japan*, **17**, 306 (1962)

[129] K. Tanaka, T. Seto and T. Hara, *J. Phys. Soc. Japan*, **17**, 873 (1962)

[130] T. Seto, T. Hara and K. Tanaka, *Jap. J. Appl. Phys.*, **7**, 31 (1968)

[131] Y. Kikuchi and S. Krimm, *J. Macromol. Sci. - Phys.*, **B4(3)**, 461 (1970)

[132] D. Chapman, *Colloq. Spectr. Intern.*, **6**, 609 (1956)

[133] R. F. Holland and J. R. Nielsen, *J. Mol. Spectrosc.*, **8**, 383 (1962)

[134] P. J. Flory, "*Statistical Mechanics of Chain Molecules*", Interscience, New York (1969)

[135] E. A. Cole and R. D. Holmes, *J. Polym. Sci.*, **46**, 245 (1960)

[136] F. A. Quinn and L. Mandelkern, *J. Am. Chem. Soc.*, **80**, 3178 (1958)

[137] A. Dahme and J. Dechant, *Acta Polym.*, **33**, 490 (1982)

[138] J. van Ruiten, F. van Dieren and V. B. F. Mathot in "*Crystallization of Polymers*", Ed., M. Dosiere, NATO ASI-C Series on Mathematical and Physical Sciences, p. 481 (1993)

[139] E. R. Walter and F. P. Reding, *J. Polym. Sci.*, **21**, 501 (1956)

[140] R. M. Eichhorn, *J. Polym. Sci.*, **31**, 197 (1958)

[141] P. R. Swan, *J. Polym. Sci.*, **56**, 409 (1962)

[142] C. H. Baker and L. Mandelkern, *Polymer*, **7**, 71 (1966)

[143] C. W. Bunn, "*Polyethylene*", Ed., A. Renfew and P. Morgan, Illife, London, Chap. 5